OCTOBER 1977

HEWLETT-PACKARD JOURNAL

Advanced Digital Signal Analyzer Probes Low-Frequency Signals with Ease and Precision

Significant new features include absolute internal calibration in the user's choice of engineering units, digital band selectable or 'zoom' analysis, fully annotated dual-trace CRT display with X and Y axis cursors, digital storage of data and measurement setups on a tape cartridge, and a random noise source to provide test stimulus.

by Richard H. Grote and H. Webber McKinney

DIGITAL SIGNAL ANALYSIS has become a widely used technique for the analysis of mechanical structures, noise, vibration, control systems, electronic networks, and many other devices and physical phenomena.

In the past, digital signal processing equipment has been expensive, difficult to move, and has required an operator that understands digital signal analysis as well as the problem to be solved. While there is a definite need for such sophisticated laboratory equipment, there is also a need for instrumentation that is less expensive, easier to use, and more portable.

Such an instrument is the new Model 5420A Digital Signal Analyzer (Fig. 1). The 5420A is a two-channel instrument that analyzes signals in the dc-to-25-kHz frequency range. The new analyzer has a two-tone dynamic range of 75 dB and amplitude flatness of 0.1 dB. Band selectable (zoom) analysis provides 0.004-Hz frequency resolution anywhere in the measurement band. The 5420A makes many powerful time domain and frequency domain measurements, including transient capture and time averaging, auto and cross correlation, histogram, linear spectrum, auto and cross spectrum, transfer function, coherence function, and impulse response. All measurements are continuously calibrated, and can be easily recalibrated in the operator's engineering units. Built-in random noise stimulus and a digital tape cartridge for storing data records and instrument set-ups make the 5420A a complete measuring system. Measurement results are displayed on a fully annotated, dual-trace, high-resolution CRT, and can be output directly to an optional X-Y recorder or digital plotter. The display provides three graphic formats and 14 choices of coordinates. The display scale can

Cover: *In a dramatic demonstration of its versatility, HP engineers used a Model 5420A Digital Signal Analyzer to determine the response and vibrational characteristics of a compound bow of the type used by tournament archers. Accelerometers mounted on the bow provided the input signals to the analyzer. (Bow provided by Jennings Compound Bow, Inc.)*

In this Issue:

Fig. 1. *Model 5420A Digital Signal Analyzer is a dual-channel instrument that analyzes signals in the dc-to-25-kHz frequency range. It makes many powerful time and frequency domain measurements, including spectrum, transfer function, and impulse response. Results are displayed on a fully annotated dual-trace CRT in any of three graphic formats and 14 choices of coordinates.*

be set either by the operator or automatically to maximize the use of the display surface.

Measurements

The new digital signal analyzer makes an extensive set of time domain and frequency domain measurements. Here is a description of each measurement and an example of where the measurement is useful.

Time Record Average. This measurement is used to average time records, or to capture transient time records. The Fourier transform (linear spectrum) of the time waveform is also provided. Time averaging is used primarily for improving the signal-to-noise ratio of time functions. A synchronous time signal is required to trigger the time average.

Autocorrelation. The primary application for the autocorrelation function is also pulling signals out of noise. However, the autocorrelation function does not require time synchronization. The disadvantage of autocorrelation is that the autocorrelation function of complex signals is difficult to interpret. As a result, this technique is mainly used for sinusoids, which are preserved under autocorrelation.

Crosscorrelation. The crosscorrelation function is mathematically similar to the autocorrelation function. However, crosscorrelation is used to determine the relationship between two signals. A major application of crosscorrelation is the determination of relative delays between two signals.

Histogram. The histogram provides an estimate of the probability density function of the incoming time waveform. The histogram can provide the operator with an indication of the statistical properties of a signal.

Linear Spectrum. The linear spectrum is the frequency domain equivalent of the time record average. The result of this measurement is a display of rms amplitude versus frequency. The linear spectrum requires time synchronization for averaging, and contains both magnitude and phase information.

Power or Auto Spectrum. This is the measurement performed by a traditional spectrum analyzer, that is, power as a function of frequency. The auto spectrum is calibrated in units of mean square for sinusoidal signals, power spectral density for random signals, or energy density for transient signals. The auto spectrum is used for characterizing signals in the frequency domain.

Cross Spectrum. The cross spectrum is the frequency domain equivalent of the crosscorrelation function. The cross spectrum produces a display of relative power versus frequency. The cross spectrum can be used to determine mutual power and phase angle as a function of frequency.

Transfer Function. The transfer function measurement characterizes a linear system in terms of gain and phase versus frequency. When the operator selects this measurement, the following measurements are also provided.

Coherence (γ^2). This function is related to the signal-to-noise ratio ($S/N = \gamma^2/(1-\gamma^2)$). It indicates the degree of causality between the output and the input

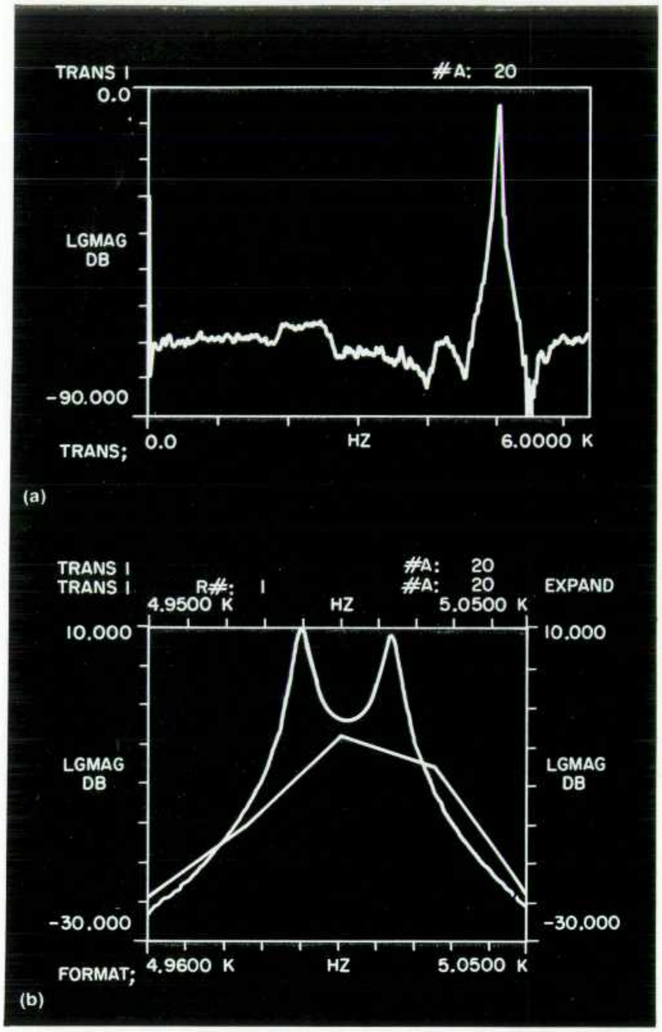

Fig. 2. *Band selectable analysis (BSA) makes it possible to zoom in on a narrow frequency band and examine the detailed structure of measured data with resolution as fine as 0.004 Hz. Here the baseband measurement (a) shows a resonance at about 5 kHz. The 0.4-Hz resolution of the BSA measurement (b) reveals that there are actually two resonances there.*

as a function of frequency. A coherence of 1 indicates perfect causality.

Input and Output Auto Spectrum. See above.

Impulse Response. The time domain equivalent of the transfer function. The impulse response shows the time response of the system to an impulsive input.

Band Selectable Analysis (BSA)

Band selectable (zoom) analysis concentrates the full resolution of the analyzer in a narrow frequency band of the user's choice. This narrow band can be placed any where in the 25-kHz bandwidth. Its width is selectable and may be less than 1 Hz. BSA can provide better than 4-mHz resolution, and measurements below 250 Hz can be made with a resolution better than 40 μHz. This resolution is obtained using purely digital techniques with no sacrifice in accuracy or dynamic range. An example of the power of BSA is shown in Fig. 2. The 25-Hz resolution of the baseband measurement of Fig. 2a indicates the presence of a single resonance centered at 5 kHz. The 0.4-Hz-resolution BSA measurement of Fig. 2b clearly shows two resonances in the vicinity of 5 kHz.

Advanced Triggering Capability

The 5420A offers the operator a wide choice of triggering capabilities, including free run, internal triggering on either channel, external triggering ac or dc coupled, and remote start.

When the analyzer is free running, it acquires and processes input data as fast as it can. For measurement bandwidths below the instrument's real-time bandwidth, this results in overlapped processing of input data. In this case, processing periods overlap input data records, and the analyzer processes the latest available data. Overlapped processing increases the variance reduction per unit time.

All triggering modes allow the operator to condition triggering by entering a per-channel pre-trigger or post-trigger delay. Pre-trigger delays up to the time record length and post-trigger delays up to 40 seconds can be accommodated. Post-trigger delays are necessary when there are inherent delays in the measurement process, such as in measuring the transfer characteristics of an auditorium. Pre-trigger delay is of particular importance when triggering on impulsive signals that have all their energy focused in a very short time interval; without pre-trigger delay it is very difficult to capture the leading edge of the signal's energy.

Easy to Use

An important design objective for the 5420A Digital Signal Analyzer was that it be easy to use, both for the novice and for the experienced operator. Front-panel design for such a powerful, flexible instrument poses particular problems. These were solved in part by using the CRT display to extend and simplify the front panel (Fig. 3). The display presents measurement parameters and status information. Instead of having to inspect all of the front-panel controls to determine how the instrument is set up, the operator simply pushes the VIEW key and the setup is displayed on the CRT. The CRT is also used to display menus of choices from which the user makes selections of measurements, averaging, input signals, and triggering.

Display Features

Once a measurement has been specified, it is initiated by pushing the START button. As soon as the first time record has been digitized and processed, fully calibrated measurement results appear on the display. If stable averaging was chosen, the measure-

Fig. 3. *CRT display extends the front panel, helping to make the new analyzer easy to use for both the novice and the experienced operator. For example, pushing the* VIEW *key causes the instrument's status to be displayed. Other keys display lists of choices from which the user can select measurement parameters.*

ment continues until the specified number of averages has been done. If one of the other averaging types —exponential, peak channel hold, or peak level hold—was selected, the instrument continues processing data and displaying calibrated results indefinitely until the operator manually stops the measurement by pushing the **PAUSE/CONT** button. Pushing this button a second time resumes the measurement by averaging new data into the previous result.

Measurement results can be viewed in any of several display formats. Fig. 2a shows the most basic **FULL** format. The instrument automatically scales and calibrates the X and Y axes, generates an internal graticule, and labels both axes. The type of measurement result—transfer function in this case—is indicated in the upper left corner of the display and the number of averages used to make the measurement is indicated in the upper right corner. In the lower left corner is an "echo field" that tells the user the last sequence of front-panel buttons pushed, and in the lower right corner are error messages, such as ADC overflow.

Two measurement results can be viewed simultaneously, either **UPPER/LOWER** (Fig. 1), or one superimposed on the other, **FRONT/BACK** (Fig. 2b). The results are fully annotated and calibrated, and either trace can be modified independently of the other. These formats are of considerable benefit for such purposes as viewing two parameters of a measurement simultaneously (e.g., magnitude and phase of a transfer function), or comparing a result with that of a previous measurement.

Results can be displayed in the following coordinate systems: magnitude of the function, phase, log magnitude, log of the horizontal axis (when log magnitude versus log frequency is selected, the result is the classical Bode plot), real part of the function, imaginary part, real part plotted versus imaginary (Nyquist plot), and log magnitude versus phase (Nichols plot, useful in control theory applications). In dual display modes, the coordinates of the two traces can be chosen independently.

Cursor Capability

A major user convenience of the 5420A is its powerful cursor capability. The instrument can display two independent cursors in each axis. The positions of the cursors are indicated at the top of the display. At the intersection of the X cursor and the waveform is an intensified point, and the value of that point on the waveform is indicated on the display along with the cursor position. Hence one application of the cursor is to indentify numerical values associated with a measurement. For example, an X axis cursor can be used to identify the amplitude at a particular frequency, or the two Y axis cursors can be used to identify what frequency components are, say, 50 dB below a peak level.

Although the cursors are primarily means of identifying specific values of a measurement result, they can be used in other ways to enhance the power and the convenience of the instrument. In conjunction with the control and setup keys, the cursors can be used to define the center frequency and bandwidth of a new measurement.

In conjunction with the display operator keys, the cursors have other uses. If an X cursor is moved to coincide with a resonance of a transfer function, the frequency and the percent critical damping of that resonance can be determined by pushing the **PEAK** key.

The Module I/O Bus (MIOB)

The module input/output bus (MIOB) is the interconnect scheme for all of the modules of the 5420A Digital Signal Analyzer (cartridge, display, filters, ADC, etc.). It consists of 16 bidirectional data lines, one handshake pair for sending commands from computer to module, and one handshake pair for everything else (status flow from module to computer and data transfers). The computer can use the bus at any time to send commands to a module. The modules must accept commands at any time. However, they may send status or send or receive data only when they "own" the bus.

To maintain high speed at the system level and controllable response time, it is necessary to reduce the hardware and software overhead required for bus access. On the hardware side, this is accomplished by using burst mode transfers from 64-word FIFO memories. On the software side, all I/O is performed using two special microcoded opcodes, XCW and XIO. The computer does not use the conventional direct memory access (DMA) hardware. DMA would be useful only during the burst portion of the data transfer. It has no facilities to control response time between bursts or to perform the buffer blocking and I/O chaining required. The microcode facility of the 21MX K-Series Computer provides far greater performance.

A time log of activity on the bus during normal system operation might look like this:

- Display sends a code word (CW) then inputs 64 words
- ADC sends CW then outputs 32 words
- Display sends CW then inputs 64 words
- Display sends CW then inputs 26 words
- Computer sends $60HZSYNC (interrupt on power line sync) to display
- Keyboard sends CW
- ADC sends CW then outputs 32 words

:

Transactions are either commands from the computer to a module or burst mode transfers initiated by a module and always beginning with a code word containing the device's name and status. This structure causes the computer to be interrupt-driven, that is, most bus transactions are initiated by a device. Normally, real-time software associated with so many devices is very complex, but again, the ability of microcode to provide just the right elementary operations keeps complexity to a minimum.

Each module (display, ADC, etc.) is controlled by a separate software module called a device control process (DCP). Each DCP appears to own the entire computer all of the time and is unaware of interrupts. Hence the DCPs can be programmed using simple in-line structures instead of complex, shared-computer, save/restore registers—interactive structures characteristic of most interrupt-driven systems. The mechanisms for this simplification are the two MIOB I/O opcodes: XCW and XIO. When an MIOB interrupt (XCW) occurs, a microcoded interrupt processor automatically saves registers, reads the code word (CW) on the bus, and branches through a table to the appropriate DCP. When it is ready to relinquish control, that DCP performs another XCW opcode, causing the interrupt branch table to be updated, registers restored, and the high-level processing resumed. This entire procedure costs the DCP only 20μs per XCW, or 20μs per interrupt.

The other special I/O opcode, XIO, is a pseudo-DMA with many embellishments. An inescapable issue whenever hardware and software meet is the mapping of data structures. The hardware designer provides a 128-word sector, an 80-word FIFO memory, or a 2K-word refresh buffer, while the software designer needs an N-byte text buffer, a 1000-word data buffer, or something else. The XIO opcode directly addresses this problem. The XIO opcode's operand is a chain of four-word control blocks that define the desired I/O transfer—for example, "output three commands, then input 50 words, then output two commands." The control blocks tell where to get the commands or data by pointing to the buffer structure, which may include fixed buffers, variable buffers (e.g., the next 50 words in a 1000-word buffer), buffers requiring blocking or unblocking (a composite buffer having many physical pieces, some perhaps deactivated), circular buffers, double buffers, or some other type. This opcode transforms what is usually implemented in dynamic real-time consuming software into static definitions of data structure. For example, the display DCP that produces the calibrated data display provides the display hardware with 64-word data bursts followed by two-word command bursts. It extracts these from seven buffers containing ASCII code, cursors, graticules, annotation, and so on. Each sub-buffer is separate, variable in length, and in its own natural format. Yet the DCP is only 15 lines of code instead of the many hundreds of lines of time-critical code normally required. Furthermore, the average data transfer bandwidth is higher than could have been obtained with DMA. It exceeds 200 kHz at system level, including amortization of all overhead (code words, invisible interrupts, other devices, interrupt latency, etc.) Conventional approaches would probably yield system level average transfer bandwidth much less than 10 kHz because of this overhead, plus that associated with sharing DMA between I/O channels and sharing I/O channels between devices, and because of the software required to convert buffer formats into DMA's linear sequential forms. There is also the general program complexity that seems to be always associated with interrupt subroutines.

A time-sequenced record of all MIOB transactions is automatically maintained by the extended I/O instructions. This trace-file capability is very useful in tracking down any I/O-related problems. Another feature, backgrounding, allows DCPs to create other software processes that run at the same time as the DCP. This allows a DCP to do time-consuming operations (e.g., scan a large buffer) without tying up the MIOB at all.

-David C. Snyder

Critical damping is a measure of the sharpness of the resonance and is equal to 1/2Q, where Q is the quality factor familiar to electrical engineers. Finally, the cursor can be used to identify the harmonics of a particular spectral component. Pushing the **HARMONIC** button causes the harmonics of the frequency component, identified by an X cursor, to be intensified on the CRT.

Display Operators

Powerful post-processing capabilities allow the user to manipulate measurement results. It is possible to add, subtract, multiply, or divide a measurement by another measurement or by a complex constant. These operators could be used, for example, to calculate the percent difference between two measurements. Using another post-processing operation, the

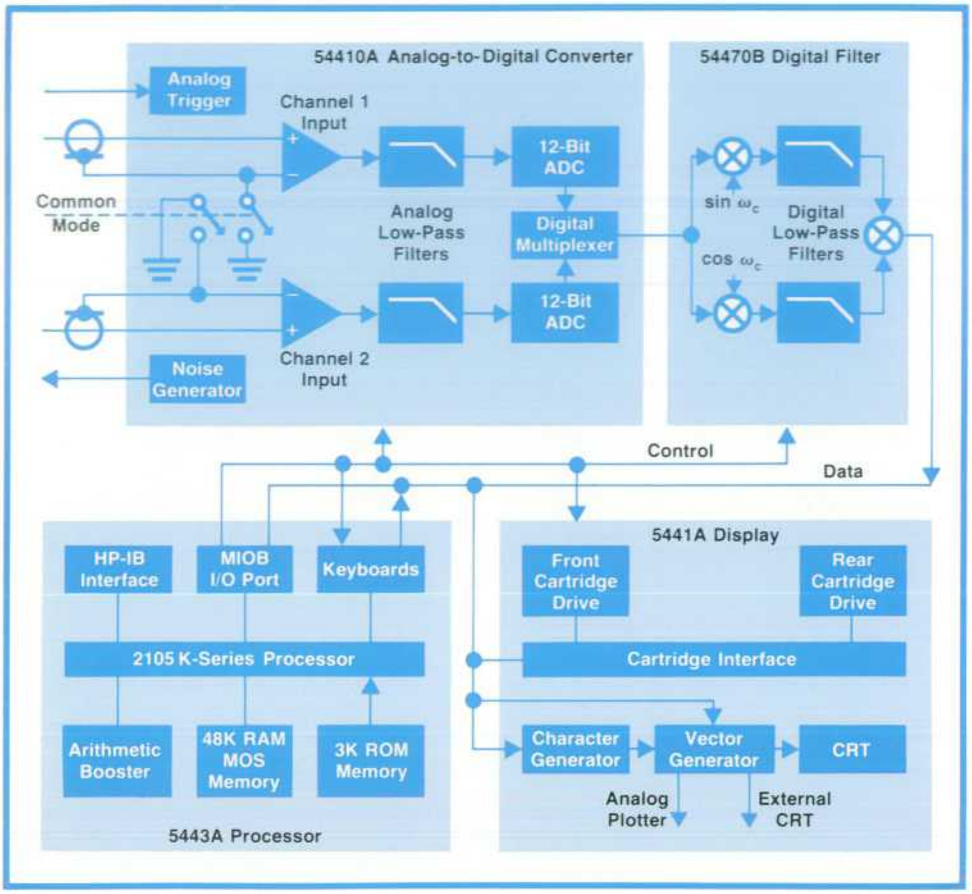

Fig. 4. *Block diagram of Model 5420A Digital Signal Analyzer. The three principal sections—central processor, analog input section, and display—are connected by a common bus. The input section consists of a dual-channel analog-to-digital converter and digital filter. An HP 21MX K-Series Computer serves as the central processor.*

user can multiply or divide a frequency domain result by $j\omega$, which has the effect of differentiating or integrating that measurement in the time domain. These operations are useful for converting acceleration spectrums to displacement spectrums, charge to current, and so forth. The **POWER** key allows the operator to calculate the total power in the display, the power at a specific line or in a band defined by the cursors, or the power in the harmonics of a particular frequency when the harmonic cursor mode is enabled. The **POWER** key turns the instrument into a frequency selective power meter.

Analyzer Organization

A block diagram of the 5420A Digital Signal Analyzer is shown in Fig. 4. The three principal elements are the central processor, the analog input section, and the display/cartridge interface section. These three functional sections are connected by a bus known as the module input/output bus (MIOB), a 50-conductor ribbon cable on the backplane of the 5420A (see box, page 6). The MIOB conveys all control and data between the processor and the input section and between the processor and the display section by means of a 16-wire parallel bus and eight control signals. By having all system I/O pass through one port of the processor, and by using only one cable, module interconnections were greatly simplified while maintaining high data transfer rates.

The processor is the central controller and data manipulator of the 5420A. The processor is a microprogrammed HP 21MX K-Series Computer with 48K words of MOS random-access memory (RAM) and 3K words of read-only memory (ROM). The ROM is used for microprogram storage. An arithmetic booster board significantly increases the computational power of the instrument. This 90-IC board bolts onto the bottom of the computer's CPU board. The MIOB interface connects the processor to the other sections of the instrument, while an HP-IB option interfaces the 5420A to the Hewlett-Packard interface bus (IEEE Standard 488-1975).

The input section consists of a dual-channel analog-to-digital converter (ADC) and digital filter. Each input channel has a floating differential input (to eliminate ground loops present in many measurement environments), anti-aliasing filters to remove unwanted spectral components above one-fourth the sampling rate, and a 12-bit successive approximation analog-to-digital converter. The input channel also has an analog trigger capable of triggering on an external signal or either of the analog inputs, and a noise generator for producing stimulus signals. The noise bandwidth is automatically adjusted to be as close as possible to the bandwidth of the measurement being made. The digital filter, which is the key to the great frequency resolution capability of the instrument, translates the frequency components of the sampled data and then digitally filters the result with one of 16 filter bandwidths.

The third section is the display and cartridge unit. The instrument has two cartridges, both interfaced through the same drive electronics. The front-panel cartridge is used for measurement results and setup state storage. Up to 120 measurement results and 50 setup states can be stored on this cartridge. The internal cartridge is used to "boot-up" the instrument at initial power turn-on. This boot-up operation is necessary because the RAM memory in the processor is volatile, so its contents need to be loaded when power is first applied.

The display is the high-resolution HP 1332A CRT with full vector and character generation circuits. An external CRT and an analog plotter can be driven directly from the connections on the rear of the display section.

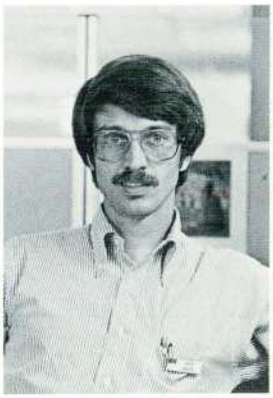

Richard H. Grote

Dick Grote has been in the digital signal analysis lab since he joined HP in 1969. Now a section manager, he was project leader for the 5420A hardware. Born in Indianapolis, Indiana, he received his BSEE degree in 1969 from the University of Kansas and his MSEE in 1971 from Stanford University. He's married to an HP mathematician (and author of a 1974 article in these pages), and lives in Palo Alto, California. His interests include woodworking and home projects, reading, old movies, singing in his church choir, and a number of sports.

H. Webber McKinney

Webb McKinney received his BSEE and MSEE degrees in 1968 and 1969 from the University of Southern California. He Joined HP in 1969 as a sales engineer, and a year later moved into the digital signal analysis lab, where he's now a section manager. He was project leader for the 5420A software and human interface. Webb was born in Upland, in southern California, and now lives in Los Altos. He spends his spare time working on his house, playing tennis, bicycling, playing folk guitar, and "getting into" yoga. He's married and has two daughters.

SPECIFICATIONS

HP Model 5420A Digital Signal Analyzer

Frequency and Time Characteristics

FREQUENCY DOMAIN:

MODES:

PASSBAND: Bandwidth (BW) about center frequency (CF).

CENTER FREQUENCY (CF): 0.016 Hz to 25 kHz, nominal.

CF SETTABILITY: Within 1.6 Hz of desired value, typically 0.016 Hz below 250 Hz.

BANDWIDTHS (BW): 16 selections from 0.8 Hz to 25 kHz for CF of 25 kHz and below. Additional 16 selections from 0.008 Hz to 250 Hz for CF of 250 Hz and below.

RANGE: $\Delta f \leq CF \pm BW/2 \leq 25$ kHz.

BASEBAND: Δf to bandwidth (BW).

CF: Specifying 0 CF selects baseband mode.

BW: Same as for passband mode.

RANGE: Same as bandwidth.

RESOLUTION (Δf): Automatically computed from bandwidth selection.

RANGE: 16 μHz to 100 Hz.

TIME DOMAIN:

TIME RECORD LENGTHS (T): 32 selections from 0.005 seconds to 32 000 seconds nominal.

RESOLUTION (Δt): Automatically computed from T.

RANGE: 10 μseconds to 64 seconds.

Measurement Characteristics

MEASUREMENTS PERFORMED:

TIME DOMAIN: View Input (Channel 1 and Channel 2); Time Average; Autocorrelation; Crosscorrelation; Impulse Response (Impulse Response is available as part of the transfer function measurement).

FREQUENCY DOMAIN: Linear Spectrum; Auto Power Spectrum; Cross Power Spectrum, Power Spectral Density, or Energy Density; High Resolution Auto Spectrum; Transfer Function; Coherence.

HISTOGRAM (Probability Density Function).

Note: Passband mode does not operate for time record, linear spectrum, or histogram measurements.

AVERAGING TYPES: All averaging types provide continuously calibrated results and may be paused, resumed, or cleared by the operator at any point in the measurement.

STABLE: Equal weighting, stops after reaching selected number of averages.

EXPONENTIAL: Stable up to number of averages selected, then exponential with decay constant equal to number of averages selected.

PEAK CHANNEL HOLD: Holds maximum value in each channel (Auto Spectrum only).

PEAK LEVEL HOLD: Holds spectrum corresponding to maximum value of cumulative channels (Auto Spectrum only).

NUMBER OF AVERAGES: From 1 to 30 000 ensemble averages.

SIGNAL TYPES:

SINUSOIDAL: Optimizes peak amplitude accuracy.

RANDOM: Normalizes power to 1 Hz noise bandwidth.

TRANSIENT: Normalizes energy to 1 Hz noise bandwidth for transient analysis.

IMPACT: Same as transient but allows preview of input signals before analysis.

CALIBRATION: All measurements are fully calibrated, including provision for a user entered calibration factor (K=C1/C2) for each channel (K1,K2) to give results in engineering units.

Measurement	Signal Type		
	Sinusoidal	Random	Transient
Auto Spectrum	$(K \cdot Vrms)^2$		$\frac{(K \cdot V)^2 sec}{Hz}$
Cross Spectrum	$K1 \cdot K2 \cdot Vrms^2$	$\frac{K1 \cdot K2 \cdot Vrms^2}{Hz}$	$\frac{K1 \cdot K2 \cdot V^2 sec}{Hz}$
Transfer Function		K2/K1	
Coherence		Unitless	
Linear Spectrum		$K \cdot Vrms$	
Time Record		$K \cdot V$	
Auto Correlation		$(K \cdot V)^2$	
Cross Correlation		$K1 \cdot K2 \cdot V^2$	
Histogram		$-K \cdot$Range to $+K \cdot$Range	

Input Characteristics

INPUT CHANNELS: Two—via BNC connectors.

INPUT IMPEDANCE:

FRONT-PANEL INPUT: 1 MΩ shunted by $<$50 pF.

REAR-PANEL INPUT: 1 MΩ shunted by $\leq$200 pF.

INPUT COUPLING:

SINGLE ENDED: dc or ac on each channel separately. Ac down 3 dB at 3 Hz nominal.

FLOATING: Differential input, dc only.

COMMON MODE REJECTION RATIO: $>$65 dB below 120 Hz for differential floating input.

MAXIMUM COMMON MODE VOLTAGE: $\pm$10 volts.

FULL-SCALE RANGES: $\pm$0.1, 0.25, 0.5, 1, 2.5, 5, and 10 volts peak.

AMPLITUDE FLATNESS: $\pm$0.1 dB over the entire frequency range ($\pm$0.05 dB typical).

CHANNEL-TO-CHANNEL MATCH:

AMPLITUDE: $\pm$0.1 dB ($\pm$0.05 dB typical).

PHASE: $\pm$5 degrees ($\pm$2 degrees typical).

TRIGGER MODES: Free run with overlap processing; internal on either input signal; external, ac or dc ($\pm$5V max level).

SLOPE: + or −

LEVEL: Adjustable from 10% to 90% of full scale.

DELAY: Independent delays on each channel, either pre- or post-trigger.

PRE-TRIGGER: $\leq$T

POST-TRIGGER: $\leq$4000T

RESOLUTION: $\pm\Delta t$

DYNAMIC RANGE: $\geq$75 dB for each full-scale range setting. Measured by taking at least 16 averages of a minimum detectable signal in the presence of a full-scale, in-band signal with random signal type selected and a frequency separation between signals of at least 6% of the selected bandwidth. Includes distortion, noise, and spurious signals caused by full-scale, outside energy within 200 kHz. For passband mode, the exact center of the passband is reduced to $\geq$65 dB from full-scale.

Noise Output Characteristics

TYPE: Broadband random, unfiltered.

BANDWIDTH:

BASEBAND MODE: dc to selected bandwidth.

PASSBAND MODE: dc to center frequency plus one-half the bandwidth, nominally.

MAXIMUM OUTPUT CURRENT: $\pm$50 mA peak.

OUTPUT LEVEL: Adjustable from 0.35 Vrms to 3.5 Vrms typically. Also 3.5 Vrms "cal" position.

CREST FACTOR: 2.5:1 typical.

Display Characteristics

NUMBER OF TRACES: One or two—designated A and B.

DISPLAY FORMATS: Full (single trace); Upper/lower (dual trace); Front/Back (dual trace).

ACTIVE TRACE: The active trace may be designated A, B, or A and B.

DISPLAY CURSORS: Cursors are displayed in full format as either a line or a band on the X axis, the Y axis, or both axes simultaneously. Cursors may be swept via their control keys or set to values explicitly entered by the operator.

DISPLAY UPDATE: Display is buffered and refreshed at the line frequency rate.

Miscellaneous Characteristics

SELF-TEST: A self-test function is provided.

HP-IB: An optional HP-IB interface is available. A rear-panel switch selects talk only or addressable operating modes. HP-IB is Hewlett-Packard's implementation of IEEE Standard 488-1975 "Digital Interface for Programmable Instrumentation."

REMOTE START: Measurement may be initiated by contact closure to ground via rear-panel BNC connector.

EXTERNAL SAMPLING: A rear-panel connector is provided for an external sampling signal at TTL levels. The frequency provided must be four times the desired range (100 kHz single, 75 kHz dual channel maximum). Internal filters may be switched out if desired.

EXTERNAL CRT OUTPUT: Horizontal, vertical and intensity outputs are provided to drive an external large screen display. Horizontal and vertical outputs provide a nominal range of $\pm\frac{1}{2}$ volt. Intensity output provides $-\frac{1}{2}$ volt to +1 volt. Display must have a 5 MHz bandwidth.

ANALOG PLOTTER OUTPUT: A rear-panel ribbon connector provides horizontal, vertical, pen-lift and servo on/off outputs to an analog plotter.

General Characteristics

DIMENSIONS: 64.14 cm (25.25 in) D × 42.55 cm (16.75 in) W × 40.64 cm (16.0 in) H.

WEIGHT: 52.16 kg (115 lbs), net.

POWER: 110V $\pm$20%, optional 230V $\pm$20%, 800 VA max. (600 watts max.), 48-66 Hz.

PRICE IN U.S.A.: $29,900.

MANUFACTURING DIVISION: SANTA CLARA DIVISION
5301 Stevens Creek Boulevard
Santa Clara, California 95050 U.S.A.

Details of the operation of these sections are described in the articles that follow.

Acknowledgments

Pete Roth originally conceived the idea for the product. Bob Puette provided support. Bob Reynolds, Al Low, and Gary Schultheis did the product design. Al Langguth designed the digitizer. Norm Rogers designed the arithmetic booster board, did microprogramming, and provided general signal processing expertise. Ralph Smith, Dave Conklin, Tom Robins, Mary Foster, and Chuck Herschkowitz developed the software. John Curlett helped with the digital filter and the front panel. Dennis Kwan and Walt Noble provided support in production. Thanks also to Bob Perdriau and Ken Ramsey for their marketing efforts, to Hal Netten, John Buck, and Richard Buchanan for manuals and service policy, and to Ken Jochim and Skip Ross for many suggestions and management talent.

Front-End Design for Digital Signal Analysis

by Jean-Pierre D. Patkay, Frank R.F. Chu, and Hans A.M. Wiggers

THE INPUT CHANNELS of the new 5420A Digital Signal Analyzer perform the dual function of data acquisition and preprocessing. Preprocessing minimizes data storage and computational demands on the central processor while providing the user with increased measurement capability.

Some signal analyzers using the Fourier transform are limited to baseband measurements, that is, the measurement band extends from dc to a maximum frequency. If increased resolution is desired, more samples must be taken, requiring more data storage and processing time. In the 5420A front end is a hardware implementation of band-selectable analysis (BSA), a measurement technique that makes it possible to perform spectral analysis over a frequency band whose upper and lower limits are independently selectable.[1] Increased resolution can be obtained by narrowing the measurement bandwidth, without increasing the data block size. BSA is realized by digitally filtering the sampled input signal to remove all data corresponding to frequencies outside the desired band.

A functional diagram of the 5420A front end is included in Fig. 4 on page 7. The hardware is divided into two plug-in modules that share a common power supply. Two analog input channels are contained in the 54410A Analog-to-Digital Converter Module. All digital filtering operations are contained in the 54470B Digital Filter Module. In combination, the two modules provide a dynamic range of 75 dB over seven input ranges from 100 mV full-scale to 10V full-scale.

A noise generator in the ADC module provides a stimulus signal for transfer function measurement. The noise generator, a combination of an analog noise source and a digital filter, generates a flat energy spectrum from dc to the maximum frequency of the measurement. The noise bandwidth tracks the selected measurement bandwidth.

The analog trigger input in the ADC module has a pseudo-logarithmic potentiometer to provide maximum trigger-level sensitivity around zero volts. Software features allow the user to advance or delay the measurement time window with respect to the trigger; this can be done independently for each channel.*

Analog Inputs

Each analog input channel has a buffered input, an anti-aliasing filter, and a 12-bit successive approximation analog-to-digital-converter (ADC). The maximum measurement frequency is determined by the sampling frequency, which is the conversion rate of the ADC, and by the anti-aliasing filter. According to the Nyquist sampling theorem, the maximum measurement frequency cannot exceed half the sampling frequency or measurement errors will occur. The anti-aliasing filters insure that there are no higher-frequency components that can fold down or alias into the measurement band as a result of the sampling process. Since they do not have an infinitely sharp cutoff, they further limit the maximum measurement frequency. In the 5420A the maximum sample rate is 102.4 kHz and the maximum measurement frequency is specified as 25.6 kHz.

Without BSA the input channel would be sampled at the lowest possible frequency that would still include the measurement band of interest. This gives maximum resolution for a fixed data block size, but requires a large number of available sample rates and

*To use this feature, both channels must be running constantly. The software determines when to take data. The trigger signal merely tells the software that the trigger condition has been satisfied.

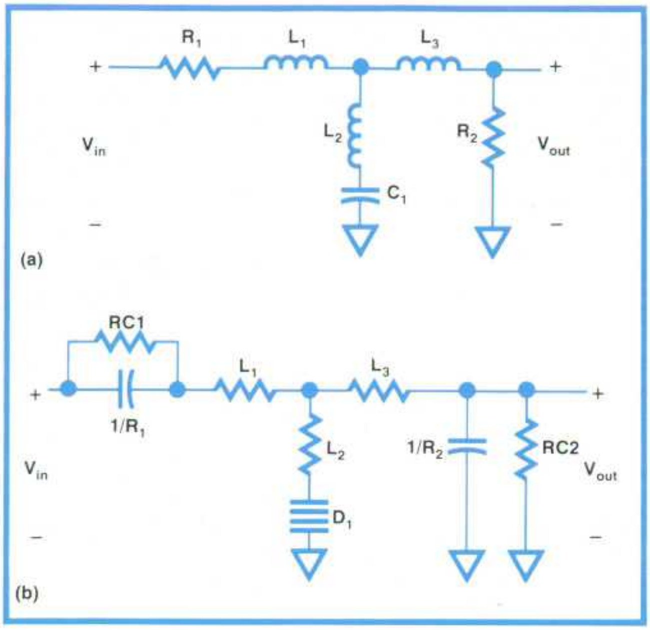

Fig. 1. *The analog anti-aliasing filters in the 5420A use the FDNR (frequency dependent negative resistance) active filter approach. Any general passive LCR network can be transformed into network of resistors, capacitors, and FDNR elements that has the same voltage transfer function. Here circuit (a) has been transformed into circuit (b). D_1 is the FDNR element. Resistors RC1 and RC2 have been added to (b) to define the dc behavior.*

either a large number of fixed filters or tracking filters, both of which are costly.

The digital filter allows us to avoid this expense. The ADC runs at only two sample rates, 102.4 kHz and 1.024 kHz, so only two anti-aliasing filter ranges are required. Higher measurement resolution in intermediate bands is obtained by means of the digital filter.

Anti-Aliasing Filters—the FDNR Approach

The two anti-aliasing filter ranges in each input channel are 30 kHz and 300 Hz. In this low frequency range, the only feasible low-pass filter type is an active filter.

The active anti-aliasing filters in the 5420A use the FDNR (frequency dependent negative resistance) approach developed by Dr. L. Bruton.[2] Basically, any general passive LCR network can be transformed into a topologically similar network that contains resistors, capacitors, and FDNR elements. The new network has the same voltage transfer function as the original LCR network. To illustrate, consider the passive LCR network shown in Fig. 1a. Let $V_{out}/V_{in} = N(s)/D(s)$.

Now let us make an impedance transformation, multiplying each component by 1/s. The transformed network is as shown in Fig. 1b. For this circuit,

$$\frac{V_{out}}{V_{in}} = \frac{N(s)/s}{D(s)/s} = \frac{N(s)}{D(s)}$$

$D_1 = 1/C_1s^2$ is the FDNR element. Resistors RC1 and RC2 are added to define the dc behavior.

The FDNR element D_1 can be realized by the circuit shown in Fig. 2. Z_{in} is a frequency dependent negative resistance.

For the 30-kHz FDNR filter used in the 5420A, the design objectives dictated a seventh-order elliptical filter with passband ripple of 0.01 dB and rejection band attenuation of 90 dB. The corresponding normalized low-pass filter is illustrated in Fig. 3.[3]

Now, for $f_c = 30$ kHz and $C = 2000$ pF, $R = 1/\omega C = 2.65\ k\Omega$. Multiplying each normalized component value by 2650 results in the FDNR filter shown in Fig. 4. This circuit has greater than 80 dB of stop-band attenuation for frequencies above 60 kHz. The passband characteristics of any two filters are matched within ±0.1 dB and phase shifts are matched within ±2° throughout the entire 5420A operating temperature range of 0°C to 50°C. The circuit components consist of high-bandwidth operational amplifiers, 1% mica dipped capacitors, and 1% metal film resistors.

Digital Filter

The digital filter can operate in two modes, a baseband mode and a passband mode. In the baseband case the band to be analyzed is between dc and some maximum frequency $f_1 \leq 25.6$ kHz,

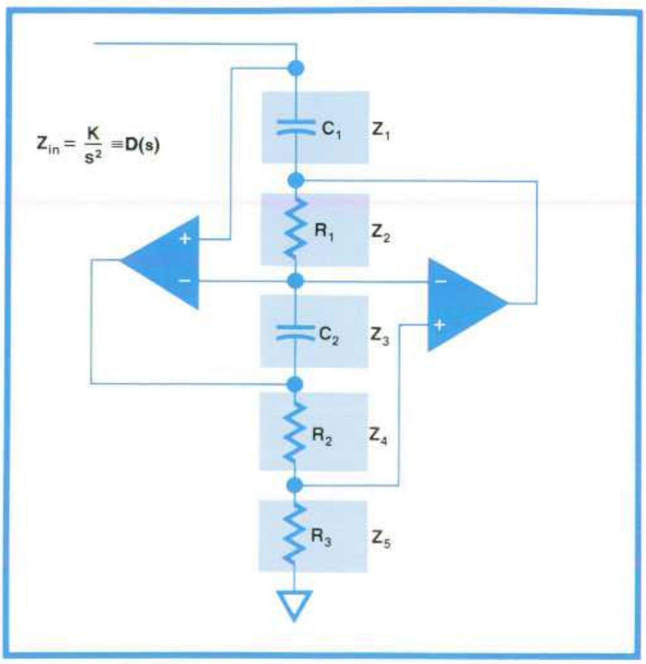

Fig. 2. *A realization of a frequency dependent negative resistance.*

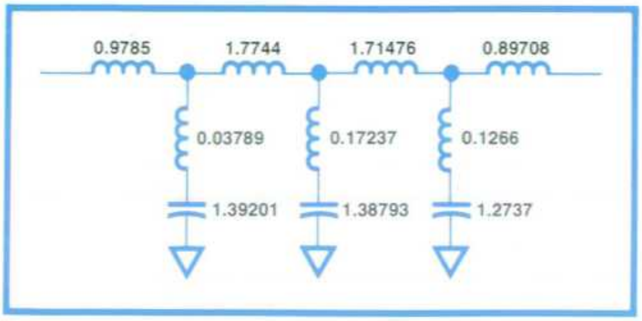

Fig. 3. *Normalized low-pass filter having the characteristics required for the 5420A's anti-aliasing filters.*

as shown in Fig. 5a. The filter is switched into the baseband mode and set to the narrowest bandwidth that includes f_1. The available bandwidths are given by

$$BW = 2^{-k} * f_s \qquad 2 \leq k \leq 17$$
$$f_s = 104.2\ \text{kHz or } 1.042\ \text{kHz}$$

This gives a total of 32 bandwidth choices.

In a more general case the user wants to analyze a band between two arbitrary frequencies f_1 and f_2, as shown in Fig. 5b. In this case the analyzer first calculates a center frequency $f_0 = ½(f_2-f_1)$, and by using the digital equivalent of a coquad mixer, shifts the entire frequency spectrum to the left by an amount f_0. This centers the desired analysis band at dc. Second, a low-pass filtering operation is used to obtain the desired bandwidth. However, there is a significant difference here from the baseband measurement. In Fig. 5a, only the positive frequency domain is shown. This is appropriate because the digital signal stream coming from the ADC represents a real signal and therefore has the property that positive and negative components are the same.[4] In the bandpass measurement, the positive and negative frequency bands are not the same, since the negative part contains the information from f_1 to f_0 and the positive part contains the information from f_0 to f_2. As a consequence, the samples describing the shifted spectrum are complex numbers instead of real ones.

This can also be seen mathematically. The effect of shifting by f_0 in the frequency domain is the same as convolving the signal with the spectral component $e^{-j\omega_0 n}$. This corresponds to multiplication of the time-domain ADC signal $x(n\Delta t)$ by $e^{-j\omega_0 t} = \cos\omega_0\Delta t - j\sin\omega_0\Delta t$, and so the shifted signal is $x(n\Delta t)\ (\cos\omega_0 n\Delta t - j\sin\ \omega_0 n\Delta t)$. Thus for every sample $x(n\Delta t)$ that goes into the frequency shifter, two components come out, a real part $x(n\Delta t)\cos\omega_0 n\Delta t$ and an imaginary part $-jx(n\Delta t)\sin\omega_0 n\Delta t$. The low-pass filter operation then has to be performed on these complex points. Fortunately, digital filtering operations are distributive, that is, filtering a complex signal is the same as filtering the real and imaginary parts separately. The frequency shift and filter operation is shown schematically in Fig. 6.

Frequency Shifter

To generate the values of $\sin\omega_0 n\Delta t$ and $\cos\omega_0 n\Delta t$ for the frequency shift operation, 1024 samples of a half-sine wave are stored in a read-only memory. The ROM address register is incremented at the sample frequency rate by an amount corresponding to ω_0. This register contains 16 bits. The two most significant bits are decoded to determine which quadrant of

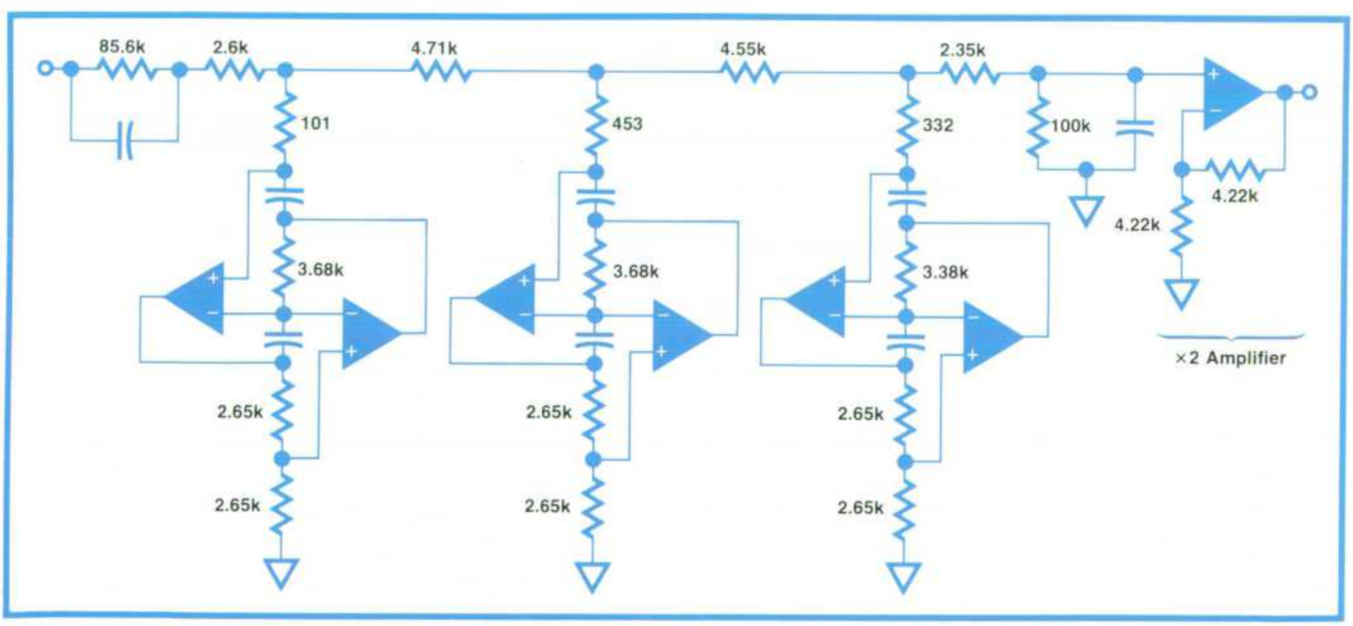

Fig. 4. *The active FDNR filter derived from the normalized filter of Fig. 3.*

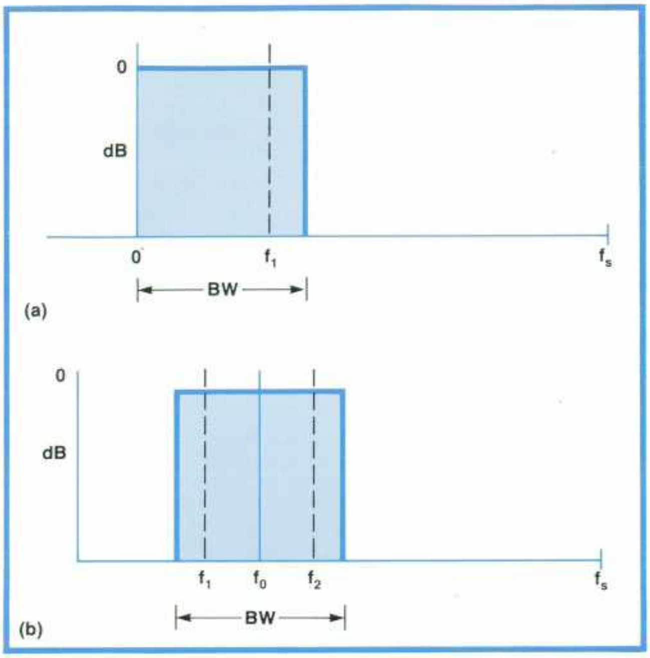

Fig. 5. *Digital band selector in the 5420A Digital Signal Analyzer operates in either baseband mode or passband mode. The user has a choice of 32 bandwidths (BW). Sampling frequency f_s is either 104.2 or 1.042 kHz.*

the sine wave the sample is in. For the first quadrant the sample stored in ROM is output. For the second quadrant the ROM address is inverted to get the correct value. For the third quadrant the value stored in ROM is used, but the output is inverted (this is done in the multiplier). For the fourth quadrant both the ROM address and the output value are inverted. To obtain the cosine samples a similar process is used.

The ADC sample and the $\cos\omega_0 t$ sample are multiplied in a hardware 12-bit×12-bit multiplier. The actual multiply takes 1.2 microseconds. A new sample can be handled every 2.4 μs, corresponding to a maximum sample rate of about 400 kHz for one channel. Since the 5420A has two channels, the maximum sample rate is 200 kHz. The actual sample rate is 102,400 samples per second, and the output of the multiplier consists of 409,600 samples per second. The digital filter has to be fast enough to handle this

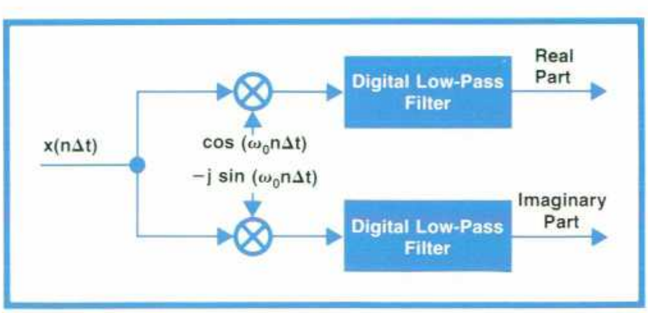

Fig. 6. *Band selectable analysis is implemented by a frequency shift and digital filtering operation.*

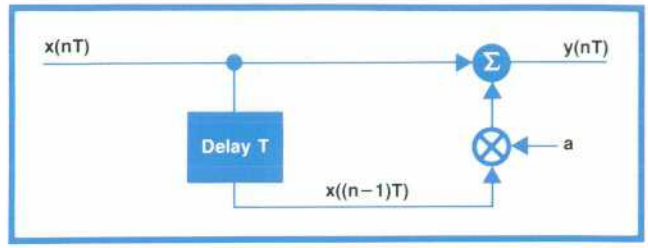

Fig. 7. *A simple first-order digital filter can be implemented with one adder, one shift register, and one multiplier.*

many samples without losing any.

Digital Filter

The digital filter is based on a linear difference system. Input samples coming from the ADC or the frequency shifter are temporarily stored in holding registers. The input samples are then combined with previous sample values to give an output value. In the simplest case (Fig. 7) the output would be $y(nt) = x(nT)+ax((n-1)T)$, which could be implemented with one adder, one shift register, and one multiplier.

Analysis of the circuit of Fig. 7 is most easily done in the frequency domain using the Fourier transform. If the Fourier transform of $x(nT)$ is $X(j\omega)$ then it can be shown that the Fourier transform of the delayed time series $x((n-1)T)$ is $e^{-j\omega T}X(j\omega)$. Thus

$$Y(j\omega) = X(j\omega) + ae^{-j\omega T}X(j\omega).$$

The transfer function of the circuit of Fig. 7 is

$$H(j\omega) = \frac{Y(j\omega)}{X(j\omega)} = 1 + ae^{-j\omega T}$$

or, using Euler's expression for $e^{-j\omega T}$,

$$H(j\omega) = 1 + a\cos\omega T - ja\sin\omega T.$$

Similar equations can be worked out for second-order difference equations. In particular, it is possible to take the delayed samples and add them to the input

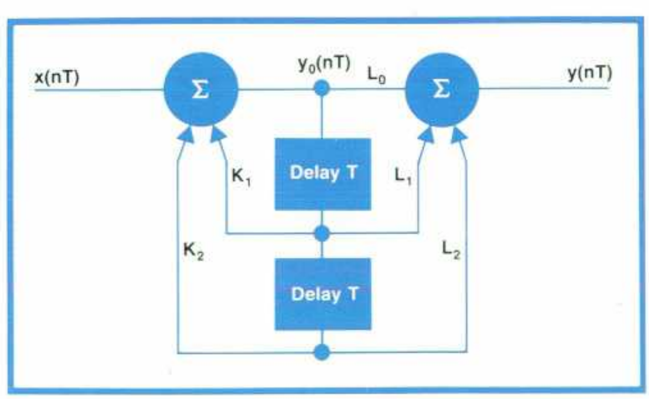

Fig. 8. *A second-order digital filter section.*

as well as to the output (see Fig. 8). The difference equations are

$$y_0(nT) = x(nT) + K_1 y_0((n-1)T) + K_2 y_0(n-2)T)$$

$$y(nT) = L_0 y_0(nT) + L_1 y_0((n-1)T) + L_2 y_0((n-2)T)$$

The transfer function is

$$H(j\omega) = \frac{Y(j\omega)}{X(j\omega)} = \frac{L \ + L\ e^{-j\omega T} + L\ e^{-2j\omega T}}{1 - K_1 e^{-j\omega T} - K_2 e^{-2j\omega T}}$$

or

$$H(j\omega) = \frac{L_0 + L_1\cos\omega T + L_2\cos 2\omega T - jL_1\sin\omega T - jL_2\sin 2\omega T}{1 - K_1\cos\omega T - K_2\cos 2\omega T + jK_1\sin\omega T + jK_2\sin 2\omega T}$$

The magnitude of this transfer function is

$$|H(j\omega)|^2 = \frac{(L_0 + L_1\cos\omega T + L_2\cos 2\omega T)^2 + (L_1\sin\omega T - L_2\sin 2\omega T)^2}{(1 - K_1\cos\omega T - K_2\cos 2\omega T)^2 + (K_1\sin\omega T + K_2\sin 2\omega T)^2}$$

at dc ($\omega = 0$),

$$|H(j\omega)| = \frac{L_0 + L_1 + L_2}{1 - K_1 - K_2}$$

The coefficients L_0, L_1, L_2, K_1 and K_2 may be selected to give unity gain at dc as well as the desired passband and rejection band characteristics.

For the 5420A, to obtain the required 80-dB out-of-band rejection, it was necessary to implement two of the sections shown in Fig. 8, each having different coefficients. The final overall filter characteristic is shown in Fig. 9.

Resampling

It should be noted that the filter characteristic is dependent on the sample frequency f_s. If f_s were twice as low, the filter passband would be twice as narrow. Also, the frequency content of the filtered signal is roughly half the content of the pre-filter signal. According to the Nyquist sampling theorem, the filter output can be resampled at half the original rate without losing information. The new sample frequency is $f_s' = \frac{1}{2}f_s$.

If this resampled signal is sent through the same filter the bandwidth is halved again. By successively filtering and resampling, the bandwidth can be reduced by powers of two. The same filter handware can be used for these consecutive steps if the filter is designed so that calculation of the first "filter pass"

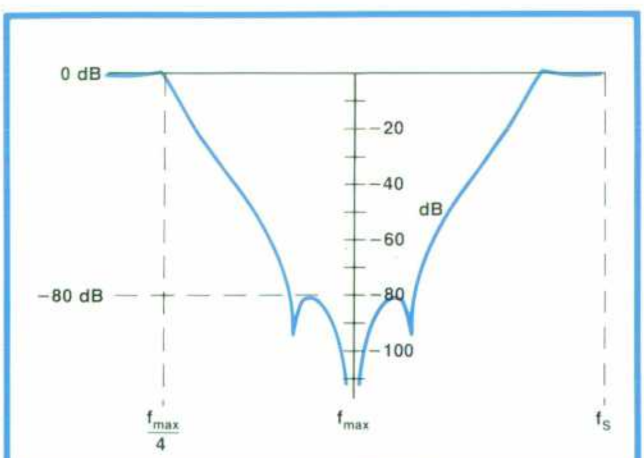

Fig. 9. *Each 5420A digital filter consists of two second-order sections and has the characteristic shown here.*

Hans A.M. Wiggers

Hans Wiggers received his engineering degree from the Technical University at Delft, The Netherlands, in 1965. He joined HP in 1972 with several years' experience in digital IC design. He designed the 54470 Digital Filter module for the 5420A. Born in Amsterdam, Hans is married, has two sons, and lives in Los Gatos, California. He's a soccer coach, an amateur photographer, and a recorder player.

Jean-Pierre D. Patkay

Pierre Patkay received BS and MS degrees in engineering from Harvey Mudd College in 1973. He Joined HP's digital signal analysis lab the same year. Pierre served as project leader and production engineer for the 54410 ADC Module for the 5420A. Born in Pasadena, California, he's married, lives in Los Altos, California, and occupies his spare time with tennis, alpine skiing, ski touring, yoga, and "pulling weeds."

Frank Rui-Feng Chu

Frank Chu designed the front end of the 54410 ADC Module and the ADC FIFO memory board for the 5420A. He's been doing circuit design for HP spectrum analyzers and digital signal analyzers since he joined the company in 1970. Frank received his BSEE degree from the University of Washington in 1970 and his MSEE degree from Stanford University in 1972. He's married, has a daughter, and lives in Santa Clara, California. He plays table tennis, collects stamps and coins, and is working on an MBA degree.

takes less than half the sample time. The other half of the available time may then be used for calculation of one of the other "passes". An algorithm to do this is built into the 5420A. The partial sums are stored in the memory instead of a shift register, and the control section regulates which pass is being calculated.

Because the digital filter must be able to handle 409,600 samples per second, and half of the time must be devoted to other passes, the maximum allowable time for one calculation is about 1.25 μs. Actually the filter performs the calculations in about half this time.

References

1. H.W. McKinney, "Band-Selectable Fourier Analysis," Hewlett-Packard Journal, April 1975.
2. L.T. Bruton, "Network Transfer Functions Using the Concept of Frequency - Dependent Negative Resistance," IEEE Transactions on Circuit Theory, Vol. CT-16, pp. 406-408, August 1969.
3. A.I. Zverev, "Handbook of Filter Synthesis," pp.278-280.
4. R.N. Bracewell, "The Fourier Transform and Its Applications," McGraw-Hill, 1965.

Display and Storage Systems for a Digital Signal Analyzer

by Walter M. Edgerley, Jr. and David C. Snyder

WHILE DATA IS BEING TAKEN into the 5420A Digital Signal Analyzer and is being manipulated by the processor, the analyzer must be displaying this data graphically and alphanumerically, without flicker, and in a clear, clean manner.

A key factor in realizing the required performance is the high-resolution HP-designed CRT. It has a viewing area of 9.6 cm × 11.9 cm and produces a keenly focused spot of 0.33 mm diameter everywhere in the viewing area, more than adequate to display alphanumeric characters 1.6 mm × 2.6 mm in size.

Data is transmitted via the MIOB (see box, page 6), which services all modules in the 5420A. The display receives data in 16-bit × 64-word bursts from the processing module. The high-speed bus makes it possible to maintain a flicker-free directed-beam display without large amounts of memory.

Fig. 1 shows the signal flow from the processor to the CRT. The data passes from the processor to the display control board via the interface and timing board. This board not only handshakes the data from the processor, but generates all timing signals for digital operations.

On the control board, the data is tested for data type, which is either graphic or alphanumeric. If graphic, it is assumed to be in horizontal and vertical pairs and is sent to the stroke generator. If alphanumeric, it is first sent to the character generator for processing into the proper horizontal and vertical bit patterns for character construction and then to the stroke generator. The stroke generator transforms the digital information into the appropriate horizontal, vertical, and blanking analog signals.

Character Generator

Fig. 2 is a block diagram of the character generator. It is an algorithmic state machine (ASM) that accepts seven-bit ASCII codes and generates appropriate horizontal and vertical bit patterns to construct the display alphanumerics. The bit pattern construction is dependent on two control lines (A and B) at the output of the ROM. There are four possible control situations:

- Load new ASCII code into ROM address register (RAR), but do not increment character counter

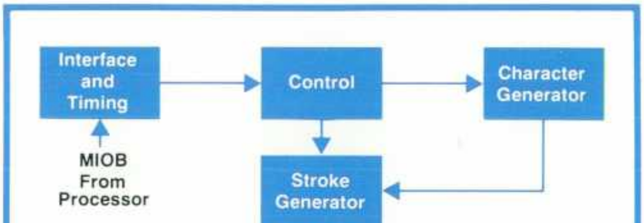

Fig. 1. *5420A display system receives data from the central processor via the MIOB and displays it on a high-resolution directed-beam CRT.*

Index

HEWLETT-PACKARD JOURNAL

Volumes 25, 26, 27, 28

September 1973 through August 1977

Hewlett-Packard Company, 1501 Page Mill Road, Palo Alto, California 94304 U.S.A.
Hewlett-Packard Central Mailing Department, Van Heuven Goedhartlaan 121, Amstelveen-1134 The Netherlands
Yokogawa-Hewlett-Packard Ltd., Shibuya-Ku, Tokyo 151 Japan

PART 1: Chronological Index

Part 1: Chronological Index (continued)

Part 1: Chronological Index (continued)

October 1975

Digital Power Meter Offers Improved Accuracy, Hands-Off Operation, Systems Compatibility, *Allen P. Edwards*

Very-Low-Level Microwave Power Measurements, *Ronald E. Pratt*

Active Probes Improve Precision of Time Interval Measurements, *Robert W. Offermann, Steven E. Schultz, and Charles R. Trimble*

Flow Control in High-Pressure Liquid Chromatography, *Helge Schrenker*

November 1975

Three New Pocket Calculators: Smaller, Less Costly, More Powerful, *Randall B. Neff and Lynn Tillman*

Inside the New Pocket Calculators, *Michael J. Cook, George Fichter, and Richard Whicker*

Packaging the New Pocket Calculators, *Thomas A. Hender*

A New Microwave Link Analyzer for Communications Systems Carrying Up to 2700 Telephone Channels, *Svend Christensen and Ian Matthews*

December 1975

A 100-MHz Analog Oscilloscope for Digital Measurements, *Allan I. Best*

An Oscilloscope Vertical-Channel Amplifier that Combines Monolithic, Thick-Film Hybrid, and Discrete Technologies, *Joe K. Millard*

A Real-Time Operating System with Multi-Terminal and Batch/Spool Capabilities, *George A. Anzinger and Adele M. Gadol*

Real-Time Executive System Manages Large Memories, *Linda W. Averett*

January 1976

An Automatic Selective Level Measuring Set for Multichannel Communications Systems, *J. Reid Urquhart*

Designing Precision into a Selective Level Measuring Set, *Hugh P. Walker*

Designing a Quiet Frequency Synthesizer for a Selective Level Measuring Set, *John H. Coster*

Making the Most of Microprocessor Control, *David G. Dack*

Real-Time Multi-User BASIC, *James T. Schultz*

February 1976

Laser Transducer Systems for High-Accuracy Machine Positioning, *André F. Rudé and Michael J. Ward*

Electronics for the Laser Transducer, *William E. Olson and Robert B. Smith*

Using a Programmable Calculator as a Data Communications Terminal, *James E. Carlson and Ronald L. Stickle*

March 1976

A Cesium Beam Frequency Reference for Severe Environments, *Charles E. Heger, Ronald C. Hyatt, and Gary A. Seavey*

Calibrated FM, Crystal Stability, and Counter Resolution for a Low-Cost Signal Generator, *Robert R. Collison and Ronald E. Kmetovicz*

A 50-Mbit/s Pattern Generator and Error Detector for Evaluating Digital Communications System Performance, *Ivan R. Young, Robert Pearson, and Peter M. Scott*

April 1976

Electronic Total Station Speeds Survey Operations, *Michael L. Bullock and Richard E. Warren*

Designing Efficiency into a Digital Processor for an Analytical Instrument, *John S. Poole and Len Bilen*

May 1976

New CRT Terminal Has Magnetic Tape Storage for Expanded Capability, *Robert G. Nordman, Richard L. Smith, and Louis A. Witkin*

Mini Data Cartridge: A Convincing Alternative for Low-Cost, Removable Storage, *Alan J. Richards*

Laboratory Notebook—A Logarithmic Counter

June 1976

Third-Generation Programmable Calculator Has Computer-Like Capabilities, *Donald E. Morris, Chris J. Christopher, Geoffrey W. Chance, and Dick B. Barney*

High-Performance NMOS LSI Processor, *William D. Eads and David S. Maitland*

Character Impact Printer Offers Maximum Printing Flexibility, *Robert B. Bump and Gary R. Paulson*

Mid-Range Calculator Delivers More Power at Lower Cost, *Douglas M. Clifford, F. Timothy Hickenlooper, and A. Craig Mortensen*

July 1976

A Direct-Reading Network Analyzer for the 500-kHz-to-1.3-GHz Frequency Range, *Hugo Vifian*

Processing Wide-Range Network Analyzer Signals for Analog and Digital Display, *William S. Lawson and David D. Sharrit*

A Precision RF Source and Down-Converter for the Model 8505A Network Analyzer, *Rolf Dalichow and Daniel R. Harkins*

August 1976

Series II General-Purpose Computer Systems: Designed for Improved Throughput and Reliability, *Leonard E. Shar*

An All-Semiconductor Memory with Fault Detection, Correction, and Logging, *Elio A. Toschi and Tak Watanabe*

HP 3000 Series II Performance Measurement, *Clifford A. Jager*

September 1976

An Easier-to-Use Variable-Persistence/Storage Oscilloscope with Brighter, Sharper Traces, *Van Harrison*

An Automatic Wide-Range Digital LCR Meter, *Satoru Hashimoto and Toshio Tamamura*

October 1976

Continuous, Non-Invasive Measurements of Arterial Blood Oxygen Levels, *Edwin B. Merrick and Thomas J. Hayes*

Laboratory Notebook—A Signal-Level Reference

An Accurate Low-Noise Discriminator

Card-Programmable Digital IC Tester Simplifies Incoming Inspection, *Eric M. Ingman*

November 1976

A Pair of Program-Compatible Personal Programmable Calculators, *Peter D. Dickinson and William E. Egbert*

Portable Scientific Calculator Has Built-In Printer, *Bernard E. Musch and Robert B. Taggart*

The New Accuracy: Making $2^3 = 8$, *Dennis W. Harms*

High-Power Solid-State 5.9-12.4-GHz Sweepers, *Louis J. Kuhlman, Jr.*

The GaAs FET in Microwave Instrumentation, *Patrick H. Wang*

December 1976

Current Tracer: A New Way to Find Low-Impedance Logic-Circuit Faults, *John F. Beckwith*

New Logic Probe Troubleshoots Many Logic Families, *Robert C. Quenelle*

A Multifunction, Multifamily Logic Pulser, *Barry Bronson and Anthony Y. Chan*

Probe Family Packaging, *David E. Gordon*

Multifamily Logic Clip Shows All Pin States Simultaneously, *Durward Priebe*

Interfacing a Parallel-Mode Logic State Analyzer to Serial Data, *Justin S. Morrill, Jr.*

January 1977

A Logic State Analyzer for Microprocessor Systems, *Jeffrey H. Smith*

Firmware for a Microprocessor Analyzer, *Thomas A. Saponas*

A Versatile, Semiautomatic Fetal Monitor for Non-Technical Users, *Erich Courtin, Walter Ruchsay, Peter Salfeld, and Heinz Sommer*

February 1977

A Fast-Reading, High-Resolution Voltmeter that Calibrates Itself Automatically, *Albert Gookin*

A High-Speed System Voltmeter for Time-Related Measurements, *John E. McDermid, James B. Vyduna, and Joseph M. Gorin*

Contemporary Design Practice in General-Purpose Digital Multimeters, *Roy D. Barker, Virgil L. Laing, Joe E. Marriott, and H. Mac Juneau*

March 1977

A New Series of Small Computer Systems, *Lee Johnson*

Part 1: Chronological Index (continued)

HP 1000 Operating System is Enhanced Real-Time Executive, *David L. Snow and Kathleen F. Hahn*
Development and Application of Microprograms in a Real-Time Environment, *Harris Dean Drake*
E-Series Doubles 21MX Performance, *Cleaborn C. Riggins*
How the E-Series Performance Was Achieved, *Scott J. Stallard*
Microprogrammed Features of the 21MX E-Series, *Thomas A. Lane*
OPNODE: Interactive Linear Circuit Design and Optimization, *William A. Rytand*
Viewpoints—John Moll on HP's Integrated Circuit Technology

April 1977

Silicon-on-Sapphire Technology Produces High-Speed Single-Chip Processor, *Bert E. Forbes*
CMOS/SOS, *David Farrington*
Miniature Oscilloscope Probes for Measurements in Crowded Circuits, *Carolyn M. Finch, Marvin F. Estes, and Lawrence A. Gammill*
A Small, Solid-State Alphanumeric Display, *John T. Uebbing, Peter B. Ashkin, and Jack L. Hines*

May 1977

Signature Analysis: A New Digital Field Service Method, *Robert A. Frohwerk*
Easy-to-Use Signature Analyzer Accurately Troubleshoots Complex Logic Circuits, *Anthony Y. Chan*
Signature Analysis—Concepts, Examples, and Guidelines, *Hans J. Nadig*
Personal Calculator Algorithms I: Square Roots, *William E. Egbert*

June 1977

A Wide-Ranging Power Supply of Compact Dimensions, *Paul W. Bailey, John W. Hyde, and William T. Walker*
Remote Programming of Power Supplies Through the HP Interface Bus, *Emery Salesky and Kent Luehman*
Coaxial Components and Accessories for Broadband Operation to 26.5 GHz, *George R. Kirkpatrick, Ronald E. Pratt, and Donald R. Chambers*
Personal Calculator Algorithms II: Trigonometric Functions, *William E. Egbert*

July 1977

Small Computer System Supports Large-Scale Multi-User APL, *Kenneth A. Van Bree*
APL Data: Virtual Workspaces and Shared Storage, *Grant J. Munsey*
APLGOL: Structured Programming Facilities for APL, *Ronald L. Johnston*
APL/3000 Summary
A Dynamic Incremental Compiler for an Interpretive Language, *Eric J. Van Dyke*
A Controller for the Dynamic Compiler, *Kenneth A. Van Bree*
Extended Control Functions for Interactive Debugging, *Kenneth A. Van Bree*
CRT Terminal Provides both APL and ASCII Operation, *Warren W. Leong*

August 1977

New 50-Megabyte Disc Drive: High Performance and Reliability from High-Technology Design, *Herbert P. Stickel*
An Individualized Pulse/Word Generator System for Subnanosecond Testing, *Christian Hentschel, Günter Riebesell, Joel Zellmer, and Volker Eberle*

PART 2: Subject Index

Month/Year		Subject	Model
		A	
Apr.	1974	Accounting system, desk-top computer	9880A
Sept.	1973	Adaptive sweep in a spectrum analyzer	3580A
May	1977	Algorithm, personal calculator, square root	—
June	1977	Algorithms, personal calculator, trigonometric	—
June	1974	Algorithmic state machine design	5345A
Apr.	1977	Alphanumeric displays, solid-state	HDSP-2000
Nov.	1975	AM-to-PM conversion, detection of	3790A
July	1974	Amplifier/power supply	6825A/6A/7A
Aug.	1974	Amplitude distortion, telephone measurements	4940A
May	1975	Amplitude distortion, telephone measurements	5453A
Nov.	1974	Amplitude/delay distortion	3770A
Feb.	1974	Analyzer, data transmission errors	1645A
Aug.	1975	Analyzer, digital pattern recognition	1620A
May	1977	Analyzer, digital signature	5004A
Oct.	1973	Analyzer, logic (serial)	5000A
Jan.	1974	Analyzer, logic state (parallel)	1601L
Aug.	1975	Analyzer, logic state	1600S
Jan.	1977	Analyzer, logic state	1611A
Nov.	1975	Analyzer, microwave link	3790A
July	1976	Analyzer, network, 0.5-1300 MHz	8505A*
Sept.	1973	Analyzer, spectrum, 5 Hz to 50 kHz, portable	3580A
May	1975	Analyzer, spectrum, 10 Hz to 13 MHz	3571A/3044A/3045A*
May	1975	Analyzer, transmission parameter	5453A
Aug.	1975	Analyzing microprocessor-based systems	1600S
Apr.	1976	Angle measurements, surveying	3810A
Apr.	1974	Angio analyzer	5693A
July	1977	APL (a programming language)	3000
July	1977	APLGOL	3000
July	1975	Applications for phase-modulated generator	86634A, 86635A
July	1975	Armed measurements, counter/timer/DVM	5328A*
Sept.	1975	ATLAS (abbreviated test language for avionics systems)	9510D, option 100 9500D, option 180
Sept.	1973	Atomic frequency standard (cesium), high-performance	5061A, option 004
Mar.	1976	Atomic frequency reference (cesium)	5062C
May	1975	Attenuator, classical problem	3571A/3044A/3045A*
May	1974	Attenuators, coaxial, step, dc-18 GHz	8495A/B 8496A/B
June	1977	Attenuators, coaxial, step, dc-26.5 GHz	8495D/K
Feb.	1977	Autocalibration in a digital voltmeter	3455A*
July	1974	Automatic exposure control for X-rays	43805
June	1974	Automatic 4-GHz frequency converter plug-in	5354A
Sept.	1975	Automatic test system programming language (ATLAS)	9510D, option 100 9500D, option 180
June	1974	Averaging, time interval, theory	5345A*
		B	
Apr.	1975	Band-selectable Fourier analysis	5451B
Jan.	1976	BASIC, real-time multi-user	92101A
Dec.	1974	BASIC/3000 timeshared computer	

*Asterisk indicates instruments compatible with the HP interface bus (HP-IB).

PART 2: Subject Index (continued)

PART 2: Subject Index (continued)

PART 2: Subject Index (continued)

PART 2: Subject Index (continued)

PART 3: Model Number Index

*Asterisk indicates instruments compatible with the HP interface bus (HP-IB).

Part 3: Model Number Index (continued)

Part 3: Model Number Index (continued)

33321D/K	Step Attenuators, dc-26.5 GHz	June 1977
33330C	Coaxial Detector, 0.01-26.5 GHz	June 1977
43805	X-Ray System	July 1974
47201A	Oximeter	Oct. 1976
*59301A	ASCII-Parallel Converter	Jan. 1975
*59303A	Digital-to-Analog Converter	Jan. 1975
*59304A	Numeric Display	Jan. 1975
*59306A	Relay Actuator	Jan. 1975
*59307A	VHF Switch	Jan. 1975
*59308A	Timing Generator	Jan. 1975
*59309A	ASCII Digital Clock	Jan. 1975
*59401A	Bus System Analyzer	Jan. 1975
*59501A	Isolated D-A/Power Supply Programmer	June 1977
62604J et al.	Switching Regulated Modular Power Supplies	Dec. 1973
62605M	500W Switching Regulated Power Supply	Apr. 1975
86242C, 86250C	RF Plug-Ins for 8620C Sweep Oscillator	Nov. 1976
86290A	2-18 GHz RF Plug-In	Mar. 1975
86603A	1-2600 MHz RF Section	July 1975
86634A	PM Modulation Section	July 1975
86635A	FM/PM Modulation Section	July 1975
91700A et al.	Distributed Computer Systems	Nov. 1974
92001A	RTE-II Real-Time Executive System	Dec. 1975
92001B	RTE-II Real-Time Executive System	Mar. 1977
92060A	RTE-III Real-Time Executive System	Dec. 1975
92060B	RTE-III Real-Time Executive System	Mar. 1977
92061A	RTE Microprogramming Package	Mar. 1977
92101A	Real-Time BASIC Subsystem	Jan. 1976
92817A	OPNODE	Mar. 1977

PART 4: Author Index

Author	Month/Year
A	
Adler, Robin	Oct. 1973
Ainsworth, Gerald	Oct. 1976
Aken, Michael B.	May 1975
Anzinger, George A.	Dec. 1975
Arnold, David	May 1976
Ashkin, Peter B.	Apr. 1977
Atchley, Robert L.	May 1975
Averett, Linda W.	Dec. 1975
B	
Bailey, Paul W.	June 1977
Baker, Mark	Oct. 1973/ Oct. 1976
Baldwin, Richard R.	Jan. 1974
Barney, Dick B.	June 1976
Barker, Roy D.	Feb. 1977
Barraclough, Hal	Dec. 1974
Basawapatna, Ganesh	Mar. 1975
Beckwith, John F.	Dec. 1976
Best, Allan I.	Dec. 1975
Bilen, Len	Apr. 1976
Blazek, Otakar	June 1975
Bologlu, Ali	June 1974/ Sept. 1975
Botka, Julius	July 1976
Bradley, Havyn E.	Apr. 1974
Brewster, John L.	July 1974
Bronson, Barry	Nov. 1974/ Dec. 1976
Buesen, Jürgen	Aug. 1975
Bullock, Michael L.	Apr. 1976
Bump, Robert B.	June 1976
C	
Campbell, John W.	Dec. 1975
Carlson, James E.	Feb. 1976
Chambers, Donald R.	June 1977
Chan, Anthony Y.	Dec. 1976/ May 1977
Chance, Geoffrey W.	June 1976
Chen, Philip	July 1976
Christensen, Svend	Nov. 1975
Christopher, Chris J.	Apr. 1974/ June 1976
Chu, Alejandro	Mar. 1975
Chu, David C.	June 1974
Clifford, Douglas M.	June 1976
Cline, Stephan G.	May 1975
Collison, Robert R.	Mar. 1976
Cornish, Eldon	Sept. 1974
Cook, Michael J.	Nov. 1975
Corya, Bruce S.	July 1975
Coster, John H.	Jan. 1976
Courtin, Erich	Jan. 1977
Crawford, Thomas	Nov. 1973
Crow, George	June 1975
D	
Dack, David G.	Jan. 1976
Dalichow, Rolf	July 1976
Damon, Noel E.	Aug. 1974
Daniels, Jerry W.	May 1975
Danielson, Dan D.	Mar. 1975
Deaver, David K.	May 1975
Dickey, Shane	Nov. 1974
Dickinson, Peter D.	Nov. 1976
Diehl, Van	Dec. 1975
Dietrich, Harold E.	Jan. 1975
DiFrancesco, Mauro	Apr. 1975
Dikeman, Peter	Apr. 1974
Dilman, Richard	Feb. 1974
DiPietro, David M.	Apr. 1975
Dresch, Donald A.	Aug. 1974
Drake, Harris Dean	Mar. 1977
Doub, James A.	June 1975
Dudley, B. William	Dec. 1973
Dudley, Robert L.	Nov. 1973
Duerr, Jeffrey R.	Feb. 1974
Dupre, John J.	Mar. 1975
E	
Eads, William D.	June 1976
Eastham, Terry	June 1975
Eberle, Volker	Aug. 1977
Edwards, Allen P.	Oct. 1975
Egbert, William E.	Nov. 1976/ May 1977/ June 1977
Eggert, Rainer	Mar. 1974
Elward, John S.	Oct. 1974
Enlow, Carl Jr.	Mar. 1975
Estes, Marvin F.	Apr. 1977
F	
Falke, Reinhard	Oct. 1973
Farnbach, William A.	Jan. 1974
Farrington, David	Apr. 1977
Felsenstein, Ronald E.	June 1974
Fichter, George	Nov. 1975
Finch, Carolyn M.	Apr. 1977
Finch, William R.	Sept. 1975
Fischer, Walter A.	Dec. 1974
Fong, Arthur	Aug. 1974
Forbes, Bert E.	Apr. 1977
Foster, Tony E.	Apr. 1974
Fowles, Richard G.	Aug. 1974
Fox, Kenneth A.	Dec. 1975
Frankenberg, Robert J.	Oct. 1974
Frederick, Wayne	July 1976
Frohwerk, Robert A.	May 1977
G	
Gadol, Adele M.	Dec. 1975
Gammill, Lawrence A.	Apr. 1977
Globas, Gert	Sept. 1974
Gookin, Albert	Feb. 1977
Gordon, David E.	Dec. 1976
Gordon, Philip	Oct. 1974
Gorin, Joseph M.	Feb. 1977
Grady, Robert B.	Sept. 1975
Graham, Thomas R.	Dec. 1973
Grote, Barbara E.	Jan. 1974
Guest, David H.	Nov. 1974/ Dec. 1974
H	
Hahn, Kathleen F.	Mar. 1977
Hale, William L.	Sept. 1973
Hall, James A.	Aug. 1974/ July 1975
Hammons, Richard L.	Oct. 1974
Hardage, P. Kent	Sept. 1974
Harkins, Daniel R.	July 1976
Harland, David A.	Jan. 1974
Harms, Dennis W.	Nov. 1976
Harrison, Joel	Aug. 1977
Harrison, Van	Sept. 1976
Hashimoto, Satoru	Sept. 1976
Hay, Robert R.	Mar. 1974
Hayes, Thomas J.	Oct. 1976
Heger, Charles E.	Mar. 1976
Heinzl, Johann J.	Aug. 1974
Hender, Thomas A.	Nov. 1975
Hentschel, Christian	Aug. 1977
Hernday, Paul R.	Mar. 1975
Hickenlooper, F. Timothy	June 1976
Hines, Jack L.	Apr. 1977
Hohmann, Hans-Günter	Feb. 1974
Hood, James M.	Dec. 1973/ Aug. 1977
Horner, James F.	July 1975
House, Charles H.	Dec. 1975
Huff, Donald W.	Feb. 1975
Hyatt, Ronald C.	Sept. 1973/ Mar. 1976
Hyde, John W.	June 1977

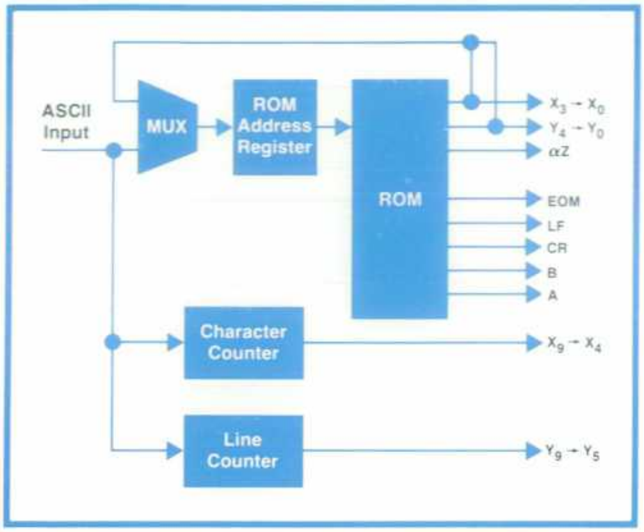

Fig. 2. *Character generator produces horizontal and vertical bit patterns for alphanumeric characters and sends them to the stroke generator.*

- Load new ROM address into RAR from ROM output
- Increment RAR to next ROM address
- Load new ASCII code into RAR and increment character counter.

These control situations allow the ASM to step consecutively from one bit pattern to the next for portions of a character that are unique, or to jump anywhere within the ROM to access portions of another character that are common to the one being constructed. For example, an eight may be made from a three and a pattern unique to an eight:

This yields maximum efficiency in the use of ROM and makes it possible to store a complete ASCII character set plus a few Greek and lower-case letters for engineering notation in 512 16-bit words of ROM.

Stroke Generator

To display high-quality lines with uniform intensity, three signals have to be generated: the horizontal component, the vertical component, and the blanking signal. This is the job of the stroke generator.

The stroke generator converts digital bit patterns into uniform line segments. The horizontal and vertical lines are voltage ramps. The blanking signal is generated from the horizontal and vertical components and determines the line's intensity and turns the beam on or off.

To generate a uniform straight line with constant intensity, the signal moving the beam should be a linear ramp, as shown in Fig. 3. A simplified diagram of the circuit used to generate this signal is shown in Fig. 4. A digital-to-analog converter (DAC) generates the desired output level. The present output value is subtracted from the DAC value to generate a difference ΔX, which is sampled and held. Then the integrator switch closes and the sample-and-hold switch opens, and the output ramps to the desired output value.

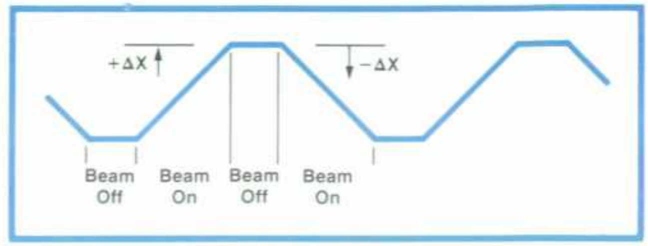

Fig. 3. *Lines are drawn by moving the beam with a smooth ramp to maintain constant intensity.*

For a given CRT drive, a certain number of electrons per second are generated by the electron gun. If the beam is moved twice as far in the same amount of time, the electron density is halved, so the line is dimmer. It is a simple matter to generate an intensity level that will compensate for this, knowing the horizontal and vertical line lengths ΔX and ΔY:

$$\text{Intensity} = A\sqrt{(\Delta X)^2 + (\Delta Y)^2},$$

where A is a proportionality constant related to the integration time.

In the 5420A, this is approximated using one-half the sum of the magnitudes of ΔX and ΔY. This results in a slightly greater intensity for horizontal and vertical lines than for diagonal lines of the same length. However, this is of little consequence, because the compensation is applied only for lines longer than a certain threshold value. In other words, some variation in intensity is permitted, although much less than there would be without compensation. This is because a slightly greater intensity for short lines than for long lines not only livens the display, but

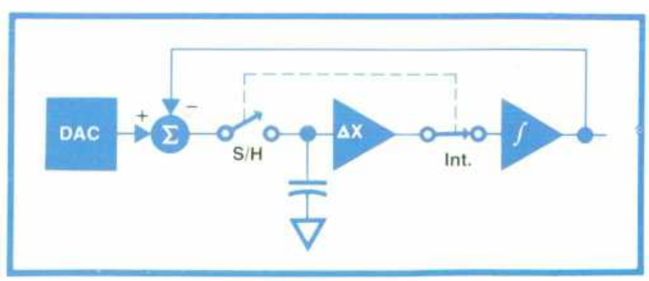

Fig. 4. *Simplified ramp generator circuit. A digital-to-analog converter generates the desired value of the output. This is subtracted from the present value and the difference is sampled and held. Then the integrator switch closes and the sample-and-hold switch opens, and the output ramps to the desired value.*

also introduces some information on how quickly a plot is changing.

Mini-Cartridge Data Storage

The mini-cartridge has proved its utility as a data storage medium in HP terminals and desktop computers.[1,2] In the 5420A Digital Signal Analyzer, the minicartridge is used for data storage and as a backup store for a large semiconductor RAM memory.

The minicartridge holds about 250,000 16-bit words of information, accessible at a 1-kHz word rate. It was designed jointly by HP and 3M corporation as a small, reliable storage device that could stand up to the vigorous demands of a computer controlled system.[3] A feature of the minicartridge is its belt drive, which eliminates tape-to-capstan contact and enhances reliability.

There are two cartridge drives in the 5420A Digital Signal Analyzer. The front-panel cartridge provides the ability to store and restore instrument setups and data waveforms for later use. The second cartridge drive is hidden under the instrument's top cover. Its function is to back up 48K words of high-speed volatile memory.

Memory Back-Up

The "personality" of the 5420A is stored in 48K words of high-speed semiconductor RAM memory. This memory is volatile, so it must be loaded during the power-up sequence. The memory loading process is accomplished in several steps and involves the 21MX K-Series Computer, a small bootstrap program residing in ROM (non-volatile), ROM-stored microcode, the module I/O bus (MIOB), and the hidden cartridge.

When the power is switched on, the computer performs an initial bootload opcode (IBL), which loads a small bootstrap program from ROM into the computer's main 48K memory. This program checks the memory and tests the integrity of the MIOB, and then proceeds to load data stored on the hidden cartridge, filling the computer's memory. To enhance reliability, the 48K memory contents are stored in 1K records, and there are multiple copies of each record on the cartridge. If an error is encountered during the loading of a record, alternate copies of the record are used. If the alternate copies also have errors, the noise reject threshold used in decoding the tape head signal is changed. Thus the loading process is desensitized

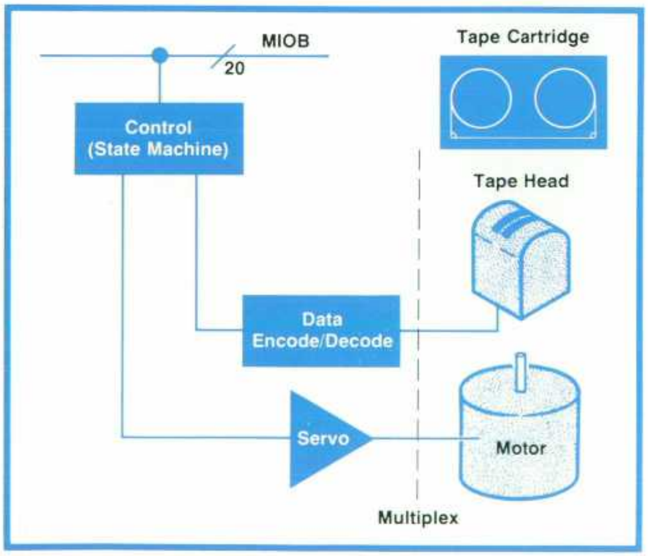

Fig. 5. *Two tape drives in the 5420A share read/write electronics and communicate with the central processor over the MIOB. One drive is used for storing data and instrument setups. The second drive is internal, and is used to back up the 5420A's semiconductor memory.*

Walter M. Edgerley, Jr.

With HP since 1971, Walt Edgerley has designed power and hybrid microwave amplifiers and, more recently, the 5441A Display Module for the 5420A. He received his BSEE degree from the University of California at Berkeley in 1972. A former professional bowler, Walt participates in a variety of sports and coaches young peoples' baseball and basketball teams. He was born in Albany, California, has two sons, and now lives in Fremont, California.

David C. Snyder

Dave Snyder designed the tape cartridge hardware and the module I/O bus for the 5420A. With HP since 1971, he's been project leader for the 5451B Fourier Analyzer and has done software design for nuclear analyzers and automatic test systems. Dave Graduated from the University of California at Berkeley with a BS degree in engineering physics in 1965. Before joining HP he worked as an astrodynamicist, a software analyst, and a software designer. He's done graduate work at three universities in a variety of fields including computer science, systems, and digital design. A native of Mankato, Minnesota, Dave is married to a nurse, has three children, and lives in the Santa Cruz mountains of California. His interests include microprocessing, games, cryptography, hiking, woodworking, photography, and guitar.

to tape errors, and in fact, will load perfectly even in the presence of multiple hard errors.

Cartridge Hardware

The cartridge hardware interfaces two tape transport assemblies, each consisting of motor, head, and preamplifier, to the 5420A module I/O bus (MIOB), as shown in Fig. 5. The MIOB transactions involve sending and receiving data, receiving commands (e.g., $RUN, $STOP, $READ,...), and sending status information (e.g., %MOVING, %EOF,...) called "code words".

The motor servo's job is to maintain the tape speed at 22 or 88 inches per second (ips), both forward and reverse. The tape velocity increases linearly from a stop to 22 ips in approximately 20 milliseconds; this corresponds to accelerating the motor uniformly from 0 to 1300 r/min within one-half of one motor revolution or about 0.5 inch of tape travel. An optical tachometer providing 2000 pulses per revolution is the control feedback element.

Data is written on the tape bit-serially, encoded in HP's delta distance format.[2] This is an efficient technique in which the recording density varies between 900 and 1600 bits per inch depending on the bit composition of the data. In this format, zeros are represented by short magnets (about 600 μin) and ones are represented by long magnets (about 1000 μin).

The control portion of the cartridge hardware handles all MIOB transactions, performs serial-to-parallel conversions, and handles exceptions (for example, sending status code words to the computer whenever an error is detected). The control section is implemented as a PROM-driven 32-state algorithmic state machine (ASM).

A diagnostic mode is provided that allows software read and write arbitrary patterns on the tape, instead of being limited to reading and writing one and zeros. Using the standard XIO pseudo-DMA opcode, the signal at the tape head may be set or sensed with a resolution of about one microsecond, equivalent to a tape motion of about 20 μin. This capability can be used to read and record worst-case test patterns such as frequency response patterns, dropout patterns, and so on, for diagnostic purposes.

References

1. R.G. Nordman, R.L. Smith, and L.A. Witkin, "New CRT Terminal Has Magnetic Tape Storage for Expanded Capability," Hewlett-Packard Journal, May 1976.
2. D.E. Morris, C.J. Christopher, G.W. Chance, and D.B. Barney, "Third-Generation Programmable Calculator Has Computer-Like Capabilities," Hewlett-Packard Journal, June 1976.
3. A.J. Richards, "Mini Data Cartridge: A Convincing Alternative for Low-Cost, Removable Storage," Hewlett-Packard Journal, May 1976.

Digital Signal Analyzer Applications

Analyses of two actual systems, one electrical and one mechanical, show what the analyzer can do.

by Terry L. Donahue and Joseph P. Oliverio

THE 5420A DIGITAL SIGNAL ANALYZER is basically a two-channel digital low-frequency spectrum and transfer function analyzer. A major application area is the analysis of mechanical structures, since these typically exhibit low-frequency (below 25 kHz) oscillations. However, its versatility, wide choice of measurements, and post-measurement processing capability make it a useful tool in other areas, such as acoustics, underwater sound, control system analysis, phase noise analysis, and filter design. This article describes two applications, one electrical, the other mechanical. The examples include the results of actual measurements made on an electronic speed controller and a mechanical structure.

Electronic Speed Controller

Fig. 1 is a block diagram of the speed controller for the 5420A's own cartridge tape drive, which is driven by an armature-controlled permanent-magnet dc motor. An analog tachometer voltage is obtained by filtering the output of an optical pulse tachometer. The set point input $R(j\omega)$ represents a command for the motor to run at a constant speed. The feedback is the analog tachometer voltage, which is proportional to motor speed and therefore tape speed. System noise, represented by $S(j\omega)$, is contributed by several elements including the unregulated dc motor voltage, mechanical imbalances in the system, and varying frictional forces.

The solid black summing node in Fig. 1 is added to the system to introduce noise $N(j\omega)$ from the 5420A's random noise source. The measurement technique is to measure the transfer function $T(j\omega)=X(j\omega)/N(j\omega)$ and compute the open-loop transfer function $G(j\omega)H(j\omega)$. This is possible because

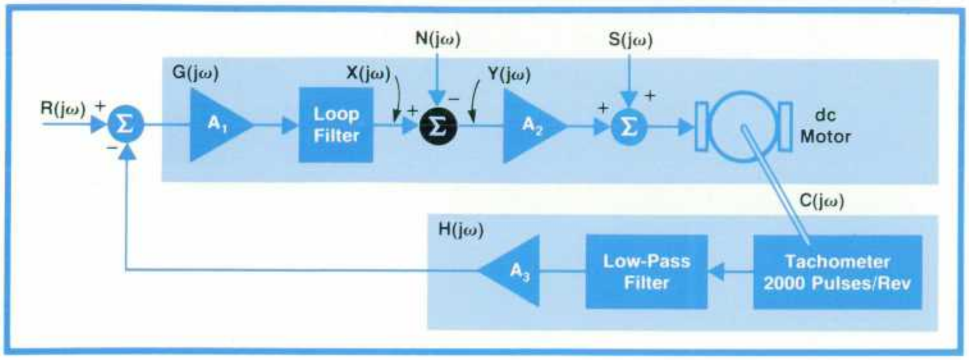

Fig. 1. *Block diagram of a cartridge tape drive system to be analyzed by the 5420A Digital Signal Analyzer. The black summing node has been added to the system to introduce noise N(jω) from the 5420A's random noise source. The technique is to measure T(jω) = X(jω)/N(jω) and compute the open-loop transfer function G(jω)H(jω).*

$T(j\omega) \approx G(j\omega)H(j\omega)/[1+G(j\omega)H(j\omega)]$.

The black summing node in Fig. 1 must be added to the system with some care. To provide isolation from the noise source and to prevent disturbing the normal operation of the system, an operational amplifier circuit, as shown in Fig. 2, can be used. The Rs should be matched to provide a gain $|Y(j\omega)/X(j\omega)|=1$ to an accuracy consistent with normal parameter variations in the system. The circuit should have unity gain and no phase shift over the control system bandwidth.

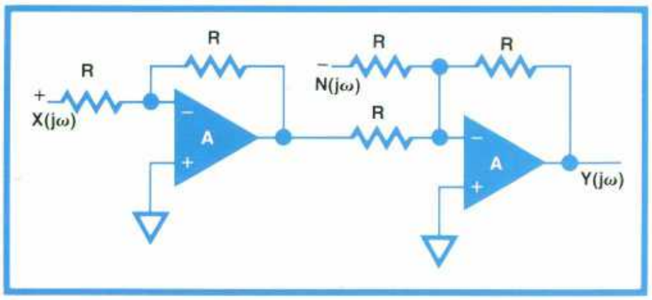

Fig. 2. *An operational amplifier circuit for introducing noise N(jω) into a system without disturbing the system.*

Fig. 3 shows log magnitude and phase versus frequency of the measured transfer function T(jω). To get the open-loop transfer function G(jω)H(jω) the 5420A's arithmetic operations are used to get the results illustrated in Fig. 4. From the figures, it is possible to estimate that G(jω)H(jω) contains a pole at 0 Hz and another at about 200 Hz. An analysis of the system predicted a response dominated by the loop filter and the motor. The loop filter was expected to contribute a pole at 0 Hz and a low-frequency zero, and the motor a low and a high-frequency pole. The measured result shows the pole at 0 Hz, the high-frequency motor pole near 200 Hz, and the low-frequency filter zero nearly perfectly cancelling the low-frequency motor pole.

Stability Analysis

Once G(jω)H(jω) has been obtained, it is possible to determine the absolute and relative stability of the system. A simplified version of the Nyquist stability criterion that can usually be applied to real systems states that a system with an open-loop transfer function G(jω)H(jω) that has no poles in the right half of the complex plane is closed-loop stable if the Nyquist plot (imaginary part versus real part) of G(jω)H(jω) for $0<\omega<\infty$ does not enclose the critical point $-1+j0$.

Fig. 5a shows the results of using the coordinate keys to display the measured G(jω)H(jω) in the Nyquist format. The system is seen to be absolutely stable since the critical point is not enclosed. Relative stability is measured by how close G(jω)H(jω) comes to enclosing the critical point. This is traditionally measured by the gain and phase margins, which are easily determined by again changing coordinates. In Fig. 5b G(jω)H(jω) is displayed using coordinates of log magnitude versus phase. The gain margin is 23 dB and the phase margin is 75 degrees.

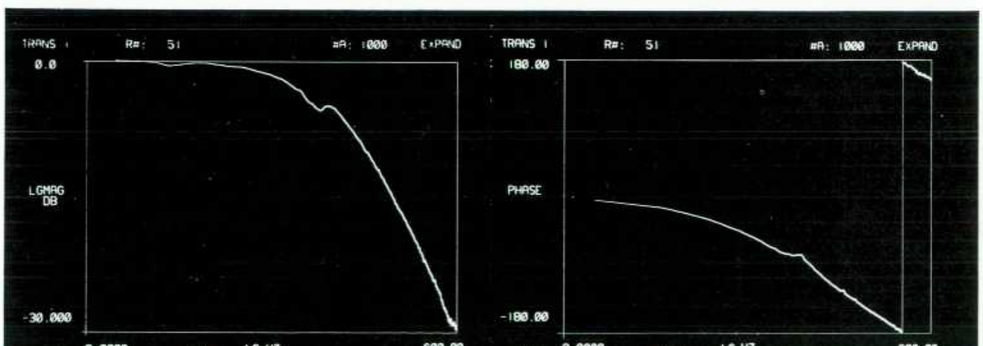

Fig. 3. *Closed-loop transfer function T(jω) measured by the 5420A.*

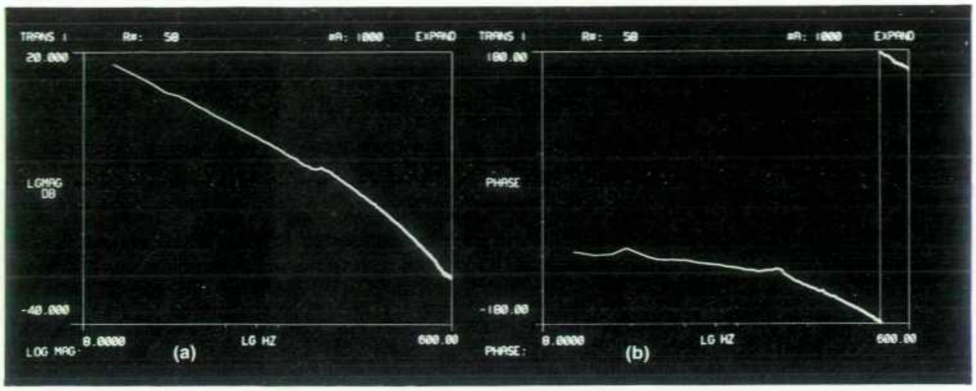

Fig. 4. *The result of calculating $G(j\omega)H(j\omega) \approx T(j\omega)/[1-T(j\omega)]$ using the 5420A's arithmetic keys.*

The measurements were repeated on the system with an extra gain block inserted into the loop. The Nyquist display is shown in Fig. 6a superimposed on the original Nyquist display. The original system is conditionally stable. Adding gain, while not making it unstable, has decreased the relative stability. From Fig. 6b, it can be seen that the gain margin has decreased to 15 dB and the phase margin to 45 degrees.

The only question remaining is the shape of the closed-loop transfer function. In the general case, this is given by $G(j\omega)/[1+G(j\omega)H(j\omega)]$. If the output of the speed controller is defined to be the tach voltage, a known function of the tape speed, the system is unity-feedback, with $H(j\omega)=1$. The closed-loop transfer function is then just $T(j\omega)$, which is shown in Fig. 3.

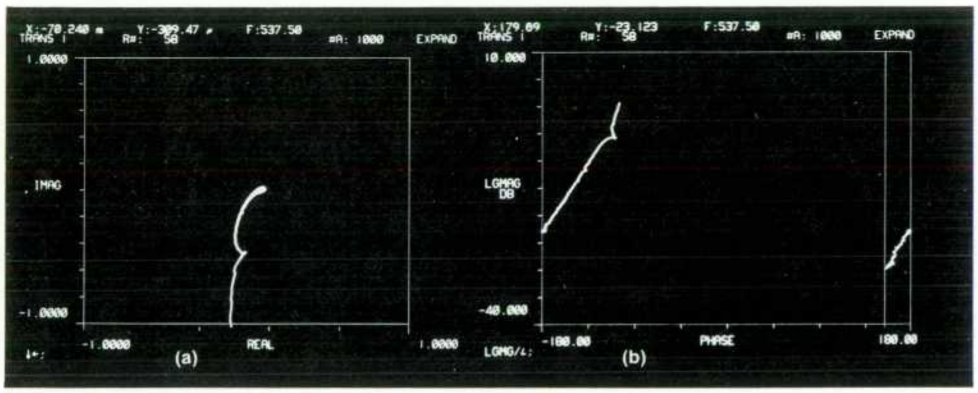

Fig. 5. *(a) Nyquist display of open-loop gain $G(j\omega)H(j\omega)$. (b) Same function in different coordinate system permits measurement of gain margin (gain at −180° phase) and phase margin (phase difference from −180° at 0 dB gain).*

Characterizing Structural Vibrations

One way of modeling the dynamic characteristics of a mechanical structure is to identify its modes of vibration. An automobile, for example, may ride smoothly at 40 mi/hr, vibrate considerably at 50 mi/hr, and then ride smoothly again at 60 mi/hr. This happens because one of the modes of vibration of the car, perhaps in the front suspension, body, or frame, is excited at 50 mi/hr but not at the other speeds. A mode is defined by a natural frequency of vibration, a damping value that defines how quickly the vibration will decay to zero when external forces are removed, and a

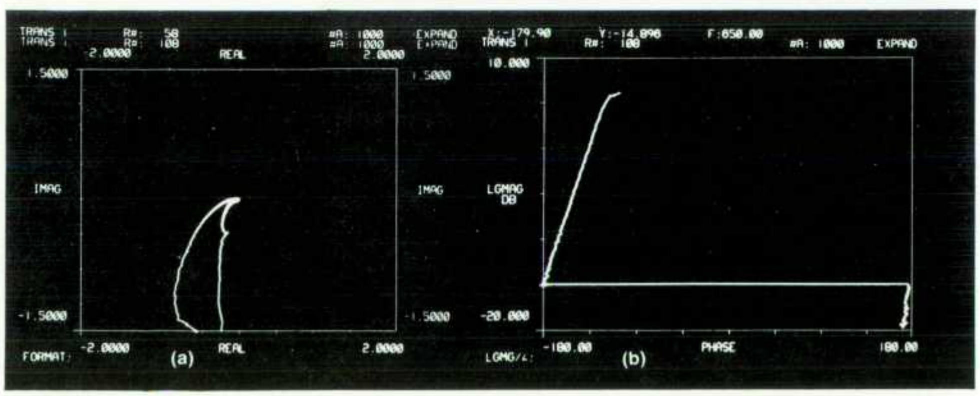

Fig. 6. *The measurements of Fig. 5 repeated with more gain in the system. Gain and phase margins have decreased.*

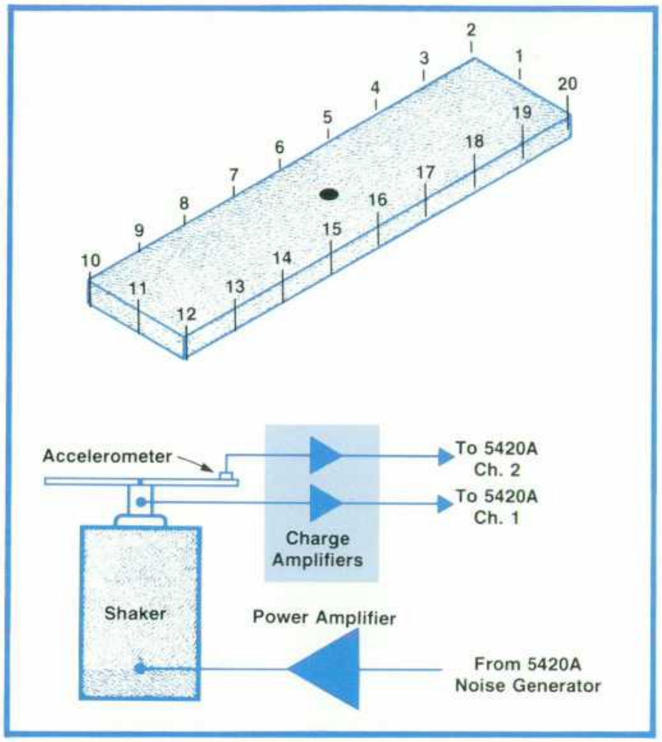

Fig. 7. *A steel plate is to be analyzed by the 5420A. An electrodynamic shaker supplies the stimulus. The plate's response is detected by accelerometers at various points on the surface.*

mode shape, or spatial distribution of the amplitude and phase of the resonant condition over the structure.

In mechanical design, one objective is to design a structure whose modes of vibration occur at frequencies outside the frequency range of known external driving forces. When this is not possible, it may be possible to add damping material to the structure, which has the effect of damping its modes of vibration as well as reducing its amplitude of vibration at any frequency.

Modal parameters—frequency, damping, and mode shape—can be identified from transfer function measurements on a structure. The following example illustrates how the 5420A can be used to identify the modes of vibration of a flat plate.

Modal Survey

The setup is shown in Fig. 7. The 5420A's noise generator is used to excite the structure by means of an electrodynamic shaker. A force transducer mounted between the structure and the shaker provides the input signal for channel 1 of the analyzer. The accelerometer mounted on the surface of the steel plate provides the response signal for channel 2 of the analyzer. The 5420A measures the transfer function of the structure between the stimulus and response points. The result is shown in Fig. 8 for position #1 on the surface. Each peak represents a mode of vibration of the structure. The resonant frequency (FR) and percent critical damping (%D) of each mode can be determined by placing the X cursor on the peak and pressing the **PEAK** key.

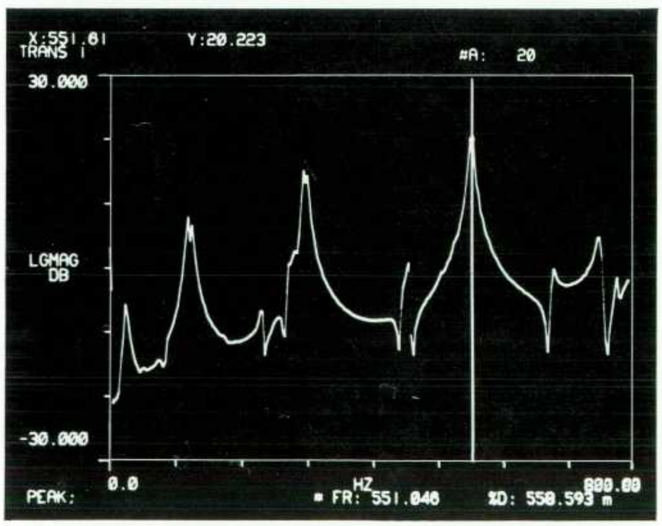

Fig. 8. *A result of the measurement of Fig. 7 for one point on the plate surface. The resonance at 551 Hz (identified by the X cursor) represents a mode of vibration with a damping factor of 0.559%.*

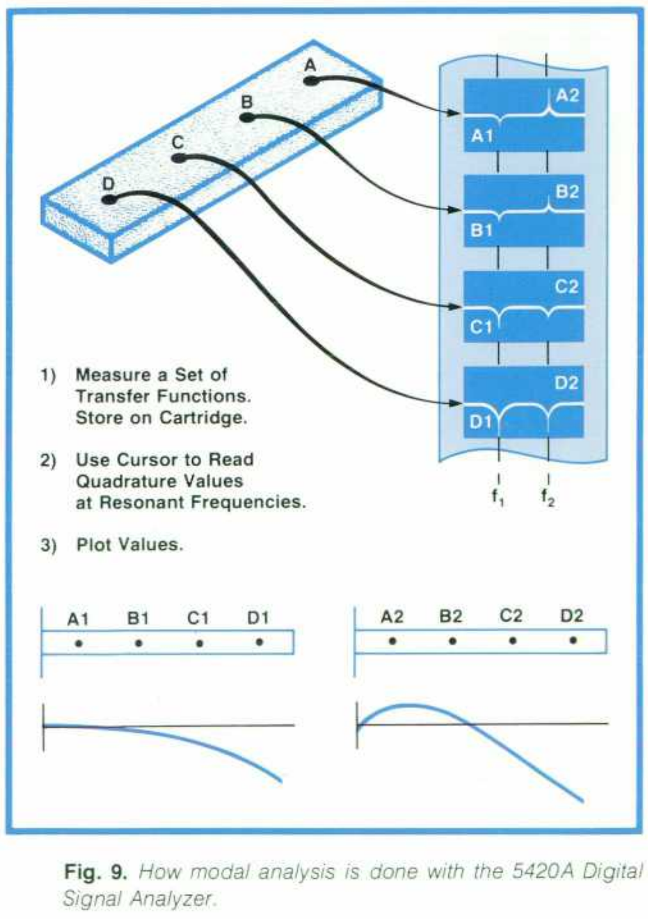

Fig. 9. *How modal analysis is done with the 5420A Digital Signal Analyzer.*

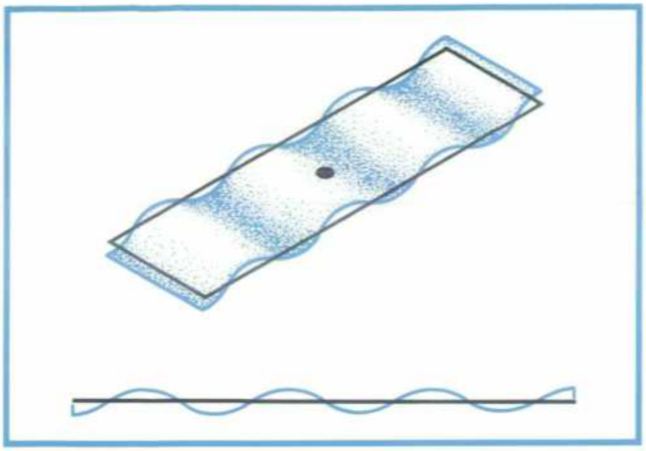

Fig. 10. *Results of a modal analysis of the steel plate.*

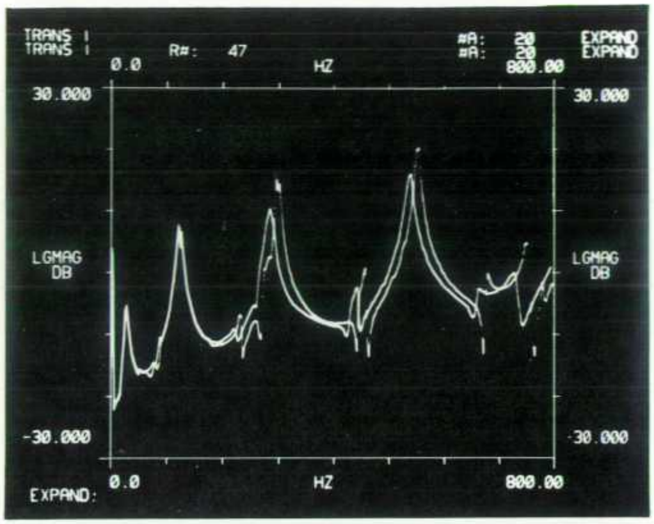

Fig. 11. *Measurements before and after adding mass to the steel plate. Extra mass decreases the amplitudes and frequencies of the resonances.*

Each response point on the structure will exhibit a different transfer function with respect to the input. For lightly damped structures the amplitude of the mode can be determined from the imaginary, or quadrature, part of the transfer function. Thus the mode shape can be drawn by recording the imaginary value of the transfer function at each measurement point for the resonance of interest and plotting these values as a function of their position on the surface. The process is shown pictorially in Fig. 9. The result of recording each imaginary value and plotting it as a function of its position on the surface is shown in Fig. 10.

Reducing Unwanted Vibrations

The two most common methods of reducing unwanted vibrations are to add mass to the structure and to increase its stiffness. Both will affect the frequency of a resonance. Adding mass will lower a natural resonant frequency. Increasing the stiffness will increase a natural resonant frequency. An example of the result of adding mass to the steel plate is shown in Fig. 11. Not only are the resonances lower in frequency but their amplitudes have decreased because the added mass increased the damping of the structure.

Joseph P. Oliverio

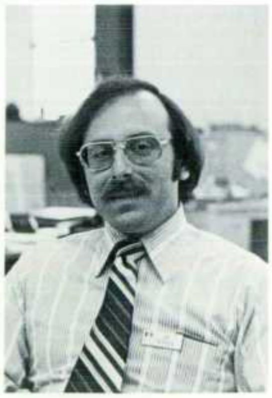

Joe Oliverio received his BSEE degree in 1968 from the University of Santa Clara. After a year as a design engineer, he joined HP in 1969 as a sales engineer. Now a digital signal analyzer product marketing engineer, he's written two magazine articles on digital signal analysis. Joe was born in San Jose, California and still lives there. He's married and has two children. He's an amateur magician and an actor in local theater productions, and he enjoys skiing, tennis, and golf.

Terry L. Donahue

Terry Donahue earned his BSEE and MSEE degrees at the University of Southern California in 1971 and 1972, and joined HP in 1972 as a design engineer. For the 5420A, he wrote the display software and compiled an application note on control system measurements. In 1976, he received his MBA degree from the University of Santa Clara. He's a member of IEEE. Terry comes from Long Beach, California. He's married and now lives in Santa Clara.

Printing Financial Calculator Sets New Standards for Accuracy and Capability

This briefcase-portable calculator has several new functions and is exceptionally easy to use. Most important, the user need not be concerned about questions of accuracy or operating limits.

by Roy E. Martin

HEWLETT-PACKARD INTRODUCED its first financial calculator, the HP-80, in 1973.[1] The HP-80 was followed, although never replaced, by the HP-81, the HP-70, the HP-22,[2] and the HP-27.

The new HP-92 Financial Calculator, Fig. 1, while superficially similar in many respects to these units, vastly exceeds all of them in functional capability and accuracy. Originally conceived as a briefcase-portable printing calculator packaged like the HP-91[3] and the HP-97[4] and having the financial capabilities of the HP-22, the HP-92 in reality goes far beyond this modest goal. Among its features are:

- Compound interest keys redefined to enhance capability and ease of use
- A printed amortization schedule, correctly rounded and clearly labeled
- Internal rate of return (IRR) that allows the user to enter up to 31 cash flows with arbitrary positive and negative values
- The greatest accuracy ever achieved in any HP financial calculator
- Calendar functions with a range of 900,000 days (approximately 2464 years)
- Bond and note functions that conform to Securities Industry Association equations[5]
- Three types of depreciation that can be done after entering data only once
- Means, standard deviations, and linear regression for two variables.

New Compound Interest Keys

The cornerstone of the HP-80 and all subsequent HP financial calculators is the row of compound interest keys: **n i PV PMT FV**

n = number of compounding periods
i = percent interest per period
PV, **PMT**, **FV** specify the cash values in various problems (**PV** = present value; **PMT** = payment; **FV** = future or final value).

These keys allow the user to solve for an unknown value by first placing known values in the calculator and then pressing the key corresponding to the unknown.

Example: Find the monthly payment due on a 36-month, 12%, $3000 loan.

	Keystrokes		
These keystrokes place the known values into the calculator	36	n	
	1	i	(12% annual is 1% per month)
	3000	PV	
Then press:		PMT	
Answer displayed:		99.64	Monthly Payment

This sequence of keystrokes will solve this problem on all previous HP financial calculators.*

The compound interest keys solve three types of problems, based on the following three equations. (In these and subsequent equations, i is a decimal fraction, e.g., 0.05 for five percent.)

$FV = PV(1+i)^n$	Compound Amount
$PV = PMT[1-(1+i)^{-n}]/i$	Loan
$FV = PMT[(1+i)^n-1]/i$	Sinking Fund

Each of these equations has four variables. As long as three of the four variables are known (n or i must be one of the three knowns) a user can solve for an unknown.

Because there are three distinct equations and only one set of keys, it is necessary to specify which equation is involved. This is done automatically through the use of status bits (flags). Internally, status bits are set when values associated with n, i, PV, PMT, FV are keyed into the calculator. As soon as three status bits are set, the equation is specified and a value can be computed.

On the HP-80, known values are pushed onto the stack and then lost when a value is computed, requiring the reentry of data on every new computation. The HP-70, HP-22, and HP-27 have separate registers to hold the financial values but require special functions to clear the status bits.

*The HP-27 requires the use of a shift key but is fundamentally the same.

Fig. 1. *HP-92 Investor is a financial printing calculator with superior accuracy and capability. Keyboard is designed to prompt the user, making many problem solutions obvious even without a manual.*

This design, although creatively conceived and cleanly implemented, is inconvenient for chained calculations. Also, an important class of problems, loans with a balance, cannot be solved without tedious iteration by the user.

The same keys, **n**, **i**, **PV**, **PMT**, **FV**, were to be on the HP-92. However, we wanted to improve and simplify their use. The most attractive alternative came in the form of a more general equation:

$$PV\,(1+i)^n + PMT\left[(1+i)^n - 1\right]/i + FV = 0.$$

The three equations in previous calculators are all special cases of this one, up to a sign change. The basic premise in this equation and a major difference between the HP-92 and other financial calculators is that money paid out is considered negative and money received is considered positive.

Implemented in the HP-92, this equation allows free-format problem solving, letting the user change any variable at any time or solve for any value at any time. It also increases the functional capability of the calculator to include loans with a balance, fixes the roles of PV, PMT, and FV, making them easier to explain, reduces the number of equations from three to one, and eliminates the need for status bits—the data in the calculator determines the problem to be solved.

In the early stages of the project, the new compound interest equation was simulated. The increase in capability and simplicity was substantial. Within minutes, inexperienced people could understand the concept and apply the keys to problems formerly considered too complicated to solve. Naturally, we were pleased. The new calculator would be more capable than earlier designs and easier to use as well. But our satisfaction was short-lived, for it turned out that here,

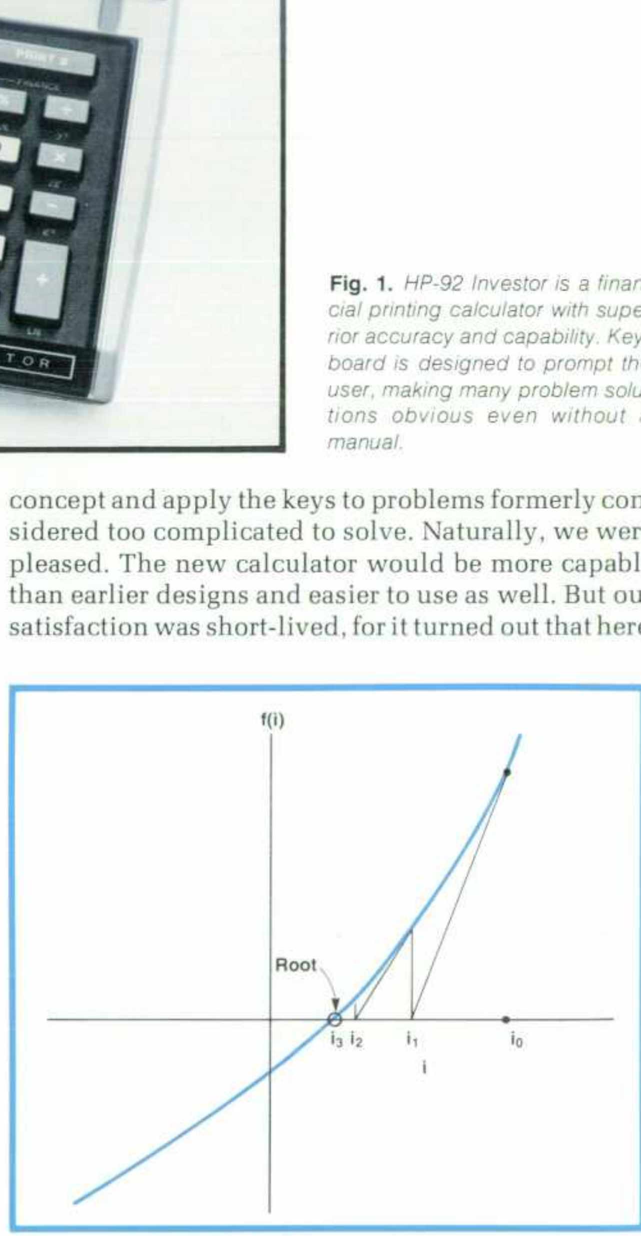

Fig. 2. *Newton's method is used by the HP-92 to solve compound interest problems. Starting from some point i_0 on the graph of an equation, the goal is to find the root of the equation, or the point where the graph crosses the axis. Drawing a tangent line to the graph at i_0 and finding where this line crosses the axis gives a second point i_1. This process is repeated to find i_2, i_3, and so on, until a point is reached that is close enough to where $f=0$. i_0 is called the initial guess.*

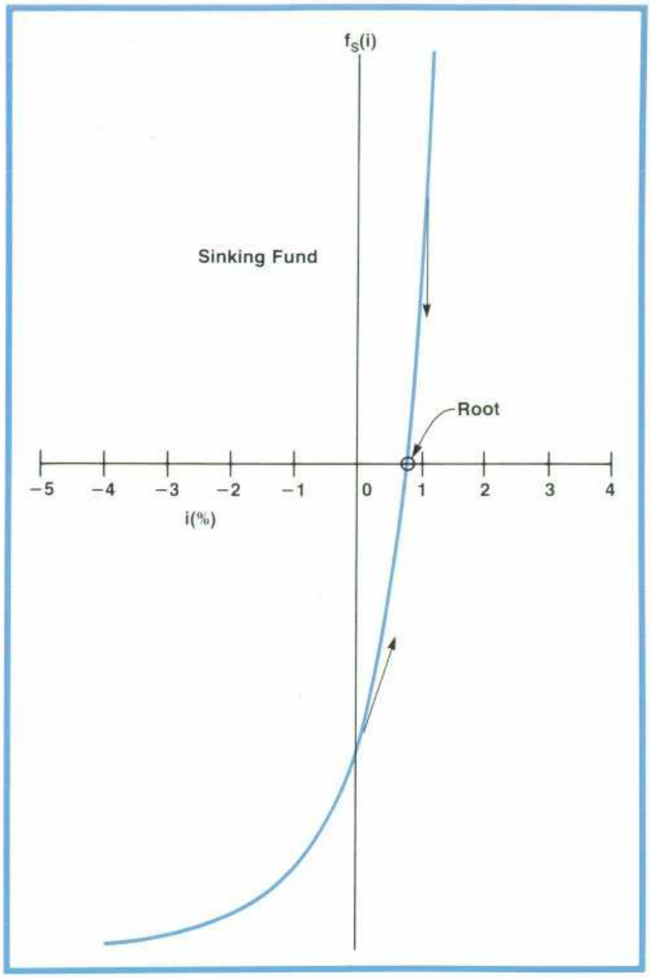

Fig. 3. *Equations used in previous HP financial calculators have favorable graph shapes (the one shown is typical), so that starting from any initial guess i_0 the steps taken by Newton's method are always toward the root.*

as usual, nothing is free.

The numerical analysis used in solving the three equations in the HP-80 had been formidable. Yet the accuracy and reliability of the algorithms was borderline and their performance deteriorated unacceptably when they were applied to the new more general equation. The most difficult problem was solving for i in the compound interest problems. Internally, this involves the microprogrammed application of Newton's method in the solution of polynomial equations (see Fig. 2).

Newton's method requires an initial guess, i_0, at the root of $f(i)=0$. Subsequent values are produced using

$$i_{k+1} = i_k + \frac{f(i_k)}{f'(i_k)}$$

until $|i_k - i_{k+1}| <$ required error limit. Basically, we slide down the graph of f(i) sawtoothing into the solution.

Three factors that affect the use of Newton's method are the shape of the graph, the accuracy of evaluation of the function f(i) and its derivative, and the quality of the initial guess. For certain graphs any reasonable initial guess will produce convergence to the correct answer. This was the case with the equations solved by previous HP financial calculators (see Fig. 3).

Inaccuracy in evaluation of the function and its derivative can cause various problems. For example, a small error can cause the iteration to step in the wrong direction, say to the previous point, resulting in an infinite loop. Worse yet, it can produce a wrong answer. The new more general equation was more sensitive than the old to round-off errors, and introduced another difficulty not encountered before.

The quality of the initial guess became a critical issue. Unless the initial guess was good enough, Newton's method would fail (see Fig. 4). With this in mind, we implemented several transformations to change the shapes of the graphs in an attempt to make Newton's iteration less sensitive to poor first guesses. We also carried extra digits and programmed numerically stable formulas to diminish the impact of rounding errors on the accuracy of intermediate calculations.

But our work was far from done. Even with the transformations and increased accuracy, initial guesses in error by less than 1% proved inadequate, because convergence was too slow when n was large.

After four months of careful examination and simu-

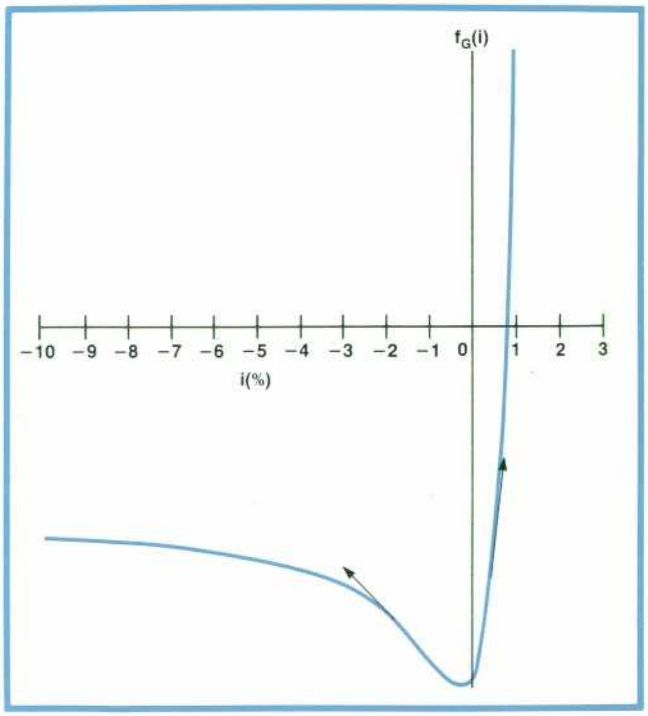

Fig. 4. *Modified equation used in HP-92 enhances ease of use, but is more difficult to solve. Shape of graph is such that some initial guesses will cause Newton's method to step away from the root. To prevent this a strategy was developed that produces initial guesses accurate to five decimal places.*

Using the n, i, PV, PMT, FV Keys

Corresponding to each of these keys is a storage register. To put a value in the storage register, just key in the value and then press the appropriate key. Money paid out is represented as negative and money received is represented as positive.

Problem:

1. If you deposit $10,000 in a fund that pays 7.75% annual rate, how much could you withdraw 12 years later?
2. If, in addition, you deposit $1000 each year thereafter, how much would you be able to withdraw after 12 years?
3. If you wanted to withdraw $45,000 at the end of the 12-year period, how much would you have to deposit each year?
4. If you could deposit $18,500 initially, how much would you have to deposit each year to be able to withdraw $45,000 at the end of the 12 years?

Solution:

Press CL FIN . This clears the registers.

1.

Key In	Then Press	Comment
12	n	This is the number of years.
7.75	i	This is the periodic interest rate.
10,000 CHS	PV	You are putting the money into the bank so you key it in as negative.
	FV	This tells the calculator that you wish to solve for the cash flow at the end of the time period.

See displayed: 24,491.05, the amount you could withdraw in 12 years.

2. After values are keyed in (or calculated), they remain in the registers. To do the second part of the problem, all we have to do is key −1000 into PMT (12 remains in n, 7.75 in i and −10,000 in PV) and then press FV

Key In	Then Press	Comment
1000 CHS	PMT	Again payment is negative because you are giving money to the bank.
	FV	This tells the calculator to find the cash flow at the end of the 12 years.

See displayed 43,189.17. The amount you could withdraw after 12 years.

3. If you needed to withdraw $45,000 and wanted to find out what your yearly deposit would be, put 45,000 into FV and then tell the calculator to solve for PMT

Key In	Then Press	Comment
45,000	FV	At the end of the 12 years you will receive $45,000.
	PMT	This tells the calculator to find the annual deposit you must make.

See displayed −1096.85. The amount you must deposit annually.

4. Now put −18,500 into PV, then press PMT

Key In	Then Press	Comment
18,500 CHS	PV	You plan to deposit $18,500 at the beginning of the 12 years.
	PMT	What will your deposit be so that you can still withdraw $45,000 at the end of 12 years?

See displayed 16.50 This tells you that you could *withdraw* this amount each year and still get $45,000 at the end of 12 years.

Fig. 5. *An example illustrating how natural the HP-92's compound interest keys are to use. An important difference from previous financial calculators is that money paid out is considered negative and money received is considered positive.*

lation we devised an initial guess strategy that produces guesses correct to five places over all ranges of PV, FV, PMT, and i, and with n as large as 10^8. Computation time for i was reduced to about a dozen seconds.

Some of the techniques employed were:

- An initial guess strategy that selects an initial guess by problem classification, the production of as many as three guesses, and the selection of the final initial guess based upon the three guesses
- Enhanced accuracy in $+$, $-$, $\times$, $\div$, ln, e^x
- Special evaluation of $[(1+i)^n-1]/i$ to avoid damage from cancellation
- Carrying more digits internally than any previous HP financial calculator.

In the final implementation of the n, i, PV, PMT, and FV keys we were able to achieve reliable functional capability over a wide range of data and problems, a dramatic enhancement in ease of use, and definitive accuracy (see accuracy discussion) exceeding that of any previous HP calculator.

Fig. 5 demonstrates how easy the new compound interest keys are to use.

Internal Rate of Return

Given an initial investment and a series of uneven cash flows CF_0, CF_1,..., CF_n occurring at equally spaced time intervals the IRR (internal rate of return) is the interest rate that satisfies the following equation:

$$CF_0+CF_1(1+i)^{-1}+CF_2(1+i)^{-2}+\ldots+CF_n(1+i)^{-n}=0.$$

The only other HP financial calculators to produce IRR are the HP-27, which allows eleven cash flows, and the HP-81, which allows ten cash flows. The HP-92 allows up to 31 uneven cash flows.

We again applied Newton's method to solve this equation, but in this case the shape of the graph presented a different type of problem. In the compound interest problem there is only one root (the graph crosses the axis only once). In the IRR problem it is possible for the equation to have many roots. Descartes' rule of signs allows polynomial equations with several changes of sign in their coefficients to have several roots. Since the cash flows in the IRR problem represent the coefficients of a polynomial (see equation), cash flows that change direction more than once produce this possibility. However, if there is more than one root, none of the solutions will be financially meaningful. To avoid this complication, the HP-27 will not allow more than one sign change.*

Example: Consider the following two problems. Negative values represent investment and positive values represent income.

	Problem 1	Problem 2
Initial	−$10,000	−$10,000
Year 1	−$ 1,000	$ 2,000
Year 2	$ 2,000	−$ 1,000
Year 3	$13,000	$13,000

The HP-27 produces an answer of 11.83% for Problem 1 but returns **ERROR** for Problem 2. To most users it is not apparent why this happens.

We wanted to remove this kind of limitation. Again

*It should be noted here that the techniques used in the HP-27 were the best available at the time. Many implementations of IRR take no precautions to protect the user from anomalous answers.

after considerable investigation we were able to implement an IRR function with a much broader range. For Problem 2 above the HP-92 produces the correct answer of 12.99%.

The IRR function on the HP-92 will produce the correct answer for any problem with up to 31 cash flows and any number of sign changes, provided that there is at least one sign change and that there is only one *significant* sign change. In general, this means that there is only one real root. Multiple sign changes are allowed provided that all but one of the cash flows changing sign are small in comparison to the other cash flows.

Example:

	Problem 3 Acceptable	Problem 4 Unacceptable
Initial	−$100,000.00	−$100,000.00
Year 1	$500.00	$500,000.00
Year 2	−$200.00	−$200,000.00
Year 3	$100.00	$100,000.00
Year 4	$150,000.00	$150,000.00

For Problem 3 the HP-92 produces the correct answer of 10.77%. For Problem 4 the HP-92 will calculate indefinitely. The mathematically correct but financially meaningless answers to Problem 4 are −147.31% and 362.98%.This does not mean that the problem is financially meaningless, but only that IRR is not the way to attack it. If there is a financially meaningful answer to an IRR problem the HP-92 will find it.

Bonds

The SIA (Securities Industry Association) handbook[5] specifies certain procedures for the calculation of bond values. Most bonds have semiannual coupon periods determined by their maturity dates. For example, if a bond matures on December 15, 1985, then the coupon periods will end on June 15, 1985, December 15, 1984, June 15, 1984, and so on. A bond is not usually purchased on a coupon date (see Fig. 6). This implies that both simple and compound interest must be used during calculations of price and yield. The SIA procedure for the calculation of purchase price involves the exact number of days in the coupon period in which the bond is purchased. The number of days in a coupon period can vary from 180 to 184. Inside the HP-92 the calendar functions determine the exact number of days to the end of the coupon period from the purchase or settlement date, automatically taking leap years into account (Fig. 7). The computations can be based on a 360 or 365-day year.

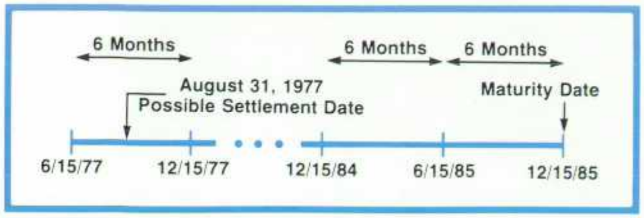

Fig. 6. *In bond calculations, coupon dates are determined by the maturity date and are six months apart. Settlement (purchase) date can be any business day. Built-in HP-92 calendar functions determine the exact number of days between the settlement date and the coupon date.*

A Manual on the Keyboard

The HP-92's keyboard is designed to prompt the user and make it obvious how to solve many problems. Keys of the same kind are grouped together. In many problems all required input parameters have individual storage registers. To place a value in one of these registers the user simply keys in the value and then presses the key corresponding to that register.

Example: There are three types of depreciation: straight line (SL), sum of the years digits (SOYD), and declining balance (DB). The input parameters and the corresponding keys are life (**LIFE**), starting period (**N1**), book value (**BOOK**), ending period (**N2**), salvage value (**SAL**), and declining balance factor (**FACT**). These values are loaded into their registers using the blue and gold shift keys where appropriate. Once this is done, any or all of the three types of depreciation schedules may be calculated by pressing the **SL**, **SOYD**, or **DB** keys.

Accuracy and Operating Limits

Everyone who participated in the HP-92's design wanted to produce a calculator whose reliability, accuracy, and capability would exceed whatever might reasonably be demanded of it. Previous calculators would have to be surpassed, if only because as time passes, users take previous accomplishments for granted and demand more. One target for improvement was accuracy. Consider the following slightly unrealistic problem.

Example: Find the present value and the future value of 63 periodic payments of one million dollars each at the (very tiny but still positive) interest rate i = 0.00000161%.

Problem:
Calculate the price of a corporate bond with a settlement date of August 24, 1977, a maturity date of March 15, 2000, a coupon rate of 8.75% and a yield of 8%. (Calculated on 30-day month, 360 day year.)
Solution:
Enter the settlement date, maturity date, coupon rate, and yield. Press **PRICE**. The bond's accumulated interest and price are then printed.

8.241977	ST
3.152000	MT
8.750000	CPN
8.000000	YLD
BOND *360	PRC
3.864583	AI
107.768456	***

Fig. 7. *A bond problem and the HP-92 solution. That February has only 28 days is automatically taken into account.*

	HP-80	HP-22,27	HP-92
PV	62,608,695.65	63,000,000.00	62,999,967.54
FV	62,608,695.65	62,981,366.46	63,000,031.44

The HP-92 answers are correct, but more significant, the other answers are clearly wrong: interest is positive but money is lost.

Obvious errors even on such unrealistic problems can undermine user confidence. The only way to prevent apprehension is to preclude all anomalies. For this reason, we set out to produce such robust algorithms that the user need never be concerned with questions of accuracy or operating limits. The extent of our success may be gauged by the reader's readiness to forget the limitations explained below.

Calendar Functions: **IS, ST, MT** Dates of issue, settlement, maturity
Δ DAYS Days between dates
DATE + DAYS
g PRINT x Day of the week.

These functions accept dates from October 15, 1582 to November 25, 4046. The first date marks the inception of the Gregorian calendar, now in use throughout Europe and the Americas, in which leap years are those evenly divisible by 4, but not by 100 unless also by 400. (The year 2000 will be a leap year, but not 1900 nor 2100.) The second date is determined by internal register limitations, not by any special knowledge of the future.

Mathematical Operations: **+, −, ×, ÷, 1/x, %, %Σ, Δ%, $\sqrt{x}$, e^x, LN**

Error is less than one unit in the last (tenth) significant digit over a range of magnitudes including 10^{-99} and 9.999999999×10^{99}. **y^x** is also accurate to within one unit in the last significant digit for $10^{-20} \leq y^x \leq 10^{20}$; outside that range the error is less than ten units in the last significant digit.

Statistics: Σ+, Σ−

These keys accumulate various sums using arithmetic to ten significant digits. This determines the range and accuracy achievable by the other statistical keys **ŷ**, **LR**, **r**, **x̄**, and **s**. For x data consisting of four-digit integers, **x̄** and **s** will be correct to ten significant digits and **ŷ**, **r**, and **LR** will be in error by less than the effect of perturbing each y value by one unit in its tenth significant digit. For x data with more than four digits per point the error can be significant if the data points have redundant leading digits; in this case both time (keystrokes) and accuracy will be conserved if the redundant digits are not entered, following recommendations by D.W. Harms.[6]

Bond Yield and Interest Rates: YIELD, i, IRR.

The error will be smaller than one unit in the last (tenth) significant digit or 0.000000001, provided that the number of periods n does not exceed 1,000,000, and for IRR, provided that the cash flows reverse sign significantly only once as described above. These rates are calculated far more accurately than the Securities Industry Association requires.

Money Values: PRICE, PMT, PV, FV, AMORT, SL, SOYD, DB, n

Errors will be smaller than the effect of changing all input values in their tenth significant digits. Typically, this means that if $(1+i)^n$ does not exceed 1000 then errors will be less than one unit in the last (tenth) digit. This amounts to a fraction of a cent in transactions involving tens of millions of dollars.

Verifying Accuracy

A simple means of verifying the accuracy of a given computation on any calculator is to attempt to recalculate the known quantities using a quantity the calculator has computed based on the knowns.

Example: Key the following values into the HP-92:

FEATURES AND SPECIFICATIONS
HP-92 Investor

MAN ALL NORM	Controls printing of keyboard operations.
BEGIN NOTE / END BOND	Selects payments at beginning or end of period; or selects bond or note calculations.
360 / 365	Day basis switch for calendar, bond/note, and interest calculations.
COMPOUND INTEREST	
n	Stores or computes number of periods.
12×	Converts number of periods from years to months.
i	Stores or computes interest rate per compounding period.
12÷	Converts interest from yearly to monthly rate.
PV	Stores or computes present value (initial cash flow at the beginning of a financial problem).
FV	Stores or computes future value (final cash flow at the end of a financial problem).
PMT	Stores or computes payment amount.
DISCOUNTED CASH FLOW ANALYSIS	
NPV	Computes net present value of future cash flows.
IRR	Computes internal rate of return of series of up to 31 cash flows.
BONDS AND NOTES	
PRICE	Stores or computes price of bond or note.
YIELD	Stores or computes yield (percentage) of a bond or note.
IS, ST	Stores the issue and settlement dates of bond or note for calculations.
MT	Stores the maturity date of a bond or note.
CALL	Stores the call price or redemption value of a bond or note.
CPN	Stores the coupon amount (percentage) for bond or note calculations.
DEPRECIATION	
SL	Calculates straight-line depreciation schedule.
SOYD	Calculates sum-of-the-years digits depreciation schedule.
DB	Calculates declining balance depreciation schedule.
BOOK	Stores book value of an asset.
LIFE	Stores depreciable life of an asset.
SAL	Stores salvage value of an asset.
N1	Stores the starting year for a depreciation schedule.
N2	Stores the ending year for a depreciation schedule.
PERCENTAGE	
%	Computes percent.
Δ%	Computes percent of change between two numbers.
%Σ	Computes percent one number is of a total.
CALENDAR	
2000 Year Calendar	October 15, 1582 to November 25, 4046.
DATE + DAYS	Computes a future or past date from a given date and a fixed number of days.
Δ DAYS	Computes number of days between dates.
g PRINT x	For a given date, prints its day of the week.
STATISTICS	
Σ+	Automatically accumulates two variables for statistics problems: Σx, Σy, Σx^2, Σy^2, Σxy, and number of terms n.
Σ−	Deletes statistical variables for changing or correction.
x̄	Computes mean for x and y.
s	Computes standard deviation for x, and y.
L.R.	Linear regression of trend line.
ŷ	Linear estimate.
r	Correlation coefficient.
STORAGE	
STO	Stores number in one of 30 storage registers. Performs storage register arithmetic upon 10 of the registers.
RCL	Recalls number from one of 30 storage registers.
PRINTING AND CLEARING	
AMORT	Prints amortization schedule.
LIST: FINANCE	Prints all values for compound interest problems, bonds and notes, and depreciation schedules.
PRINT x	Prints contents of display.
LIST: STACK	Prints contents of operational stack.
LIST: REG Σ	Together print contents of 30 addressable storage registers.
CLx	Clears display.
CL FIN	Clears financial functions for new problem.
CL REG CL Σ	Together clear 30 addressable storage registers.
CLEAR	Clears entire calculator—display, operational stack, all storage registers, and financial functions.
NUMBER ENTRY AND MANIPULATION	
ENTER↑	Separates numbers for arithmetic and other functions.
CHS	Changes sign of displayed number of exponent.
x⇄y R↓ R↑	Functions to manipulate numbers in operational stack.
EEX	Enter exponent of 10.
RND	Rounds actual number in display to number seen in display.
LAST x	Recalls number displayed before last operation back to display.
MATHEMATICS	
y^x	Raises number to power.
e^x	Natural antilogarithm.
LN	Natural logarithm.
$\sqrt{x}$	Square root.
1/x	Reciprocal.
+ − × ÷	Arithmetic functions.

PHYSICAL SPECIFICATIONS
WIDTH: 22.9 centimetres (9.0 in).
LENGTH: 20.3 centimetres (8.0 in).
HEIGHT: 6.35 centimetres (2.5 in).
WEIGHT: 1.13 kilograms (40 oz).
RECHARGER/AC ADAPTER WEIGHT: 170 grams (6 oz).
SHIPPING WEIGHT: 2.7 kilograms (5 lb 15 oz).

TEMPERATURE SPECIFICATIONS
OPERATING TEMPERATURE RANGE: 0° to 45°C (32°F to 113°F), with paper, 5% to 95% relative humidity.
CHARGING TEMPERATURE RANGE: 15° to 40°C (59° to 104°F).
STORAGE TEMPERATURE RANGE: −40° to +55°C (−40° to +131°F).

POWER SPECIFICATIONS
AC: Depending on recharger/ac adapter chosen, 115 or 230V ±10%, 50 to 60 Hz.
BATTERY: 5.0 Vdc nickel-cadmium battery pack.
BATTERY OPERATING TIME: 3 to 7 hours.
BATTERY RECHARGING TIME: Calculator off, 7 to 10 hours; calculator on, 17 hours.

PRICE IN U.S.A.: $625.

MANUFACTURING DIVISION: CORVALLIS DIVISION
1000 N.E. Circle Boulevard
Corvallis, Oregon 97330 U.S.A.

n=111.1111111, i=2.222222222, PV=333.3333333, PMT=4.444444444. These numbers are selected to make any loss of digits noticeable, but are otherwise arbitrary.

Now solve for FV. The HP-92 gives FV= −5931.82294. Now recalculate the known quantities. The HP-92 answers are n=111.1111111, i= 2.222222222, PV=333.3333333, PMT=4.444444443. Note the loss of one digit in the last place of PMT. Then resolve for FV. The HP-92 again gives FV= −5931.82294, showing that the lost digit has no impact.

Acknowledgments

The HP-92 represents the efforts and contributions of many people drawing upon technical advances in the mathematics of finance as well as in materials, mechanics, and electronics.

The bulk of the development was done by Paul Williams and me. The algorithms are based primarily on work done by Professor W. Kahan of the University of California at Berkeley. The product, as it is now defined, would never have been implemented without the early leadership and creative contributions of Bernie Musch. The hard work and enthusiasm of the following people contributed much to the total product and they can take pride in their extensive contributions: Jim Abrams (manual), Janet Cryer (applications book), A.J. Laymon, Dennis Harms, Hank Suchorski, Bob Youden, Bill Crowley, and John van Santen. I would also like to thank Bob Dudley for his support and encouragement.

References

1. W.L. Crowley and F. Rodé, "A Pocket-Sized Answer Machine for Business and Finance," Hewlett-Packard Journal, May 1973.

2. R.B. Neff and L. Tillman, "Three New Pocket Calculators: Smaller, Less Costly, More Powerful," Hewlett-Packard Journal, November 1975.

3. B. E. Musch and R. B. Taggart, "Portable Scientific Calculator has Built-In-Printer," Hewlett-Packard Journal, November 1976.

4. P. D. Dickinson and W. E. Egbert, "A Pair of Program-Compatible Personal Programmable Calculators," Hewlett-Packard Journal, November 1976.

5. B. M. Spence, J. Y. Graudenz, and J. J. Lynch, Jr., "Standard Securities Calculation Methods—Current Formulas for Price and Yield Computations," Securities Industry Association, New York, 1973.

6. D. W. Harms, "The New Accuracy: Making $2^3=8$," Hewlett-Packard Journal, November 1976.

Roy E. Martin

Roy Martin did product definition, microprogramming, and numerical analysis for the HP-92. A native Californian, he was born in San Mateo, and received his BA degree in mathematics from San Jose State University in 1967. After two years as a programmer/analyst, he enrolled at Iowa State University and received his MS degree in mathematics in 1971. He remained at Iowa State for the next two years, doing course work and teaching mathematics, then joined HP in 1973. He's worked in product support as well as the lab, and is currently doing computer performance modeling and analysis. In 1975 he conceived and wrote the script for an HP videotape that was judged best instructional videotape in the nation by the Industrial Television Association. Roy is married, has three children, and lives in San Jose. He coaches a youth soccer team and participates in a number of sports.

Hewlett-Packard Company, 1501 Page Mill Road, Palo Alto, California 94304

HEWLETT-PACKARD JOURNAL

OCTOBER 1977 Volume 29 • Number 2

Technical information from the Laboratories of Hewlett-Packard Company

Hewlett-Packard Central Mailing Department
Van Heuven Goedhartlaan 121
Amstelveen-1134 The Netherlands
Yokogawa-Hewlett-Packard Ltd., Shibuya-Ku
Tokyo 151 Japan

Editorial Director • Howard L. Roberts
Managing Editor • Richard P. Dolan
Art Director, Photographer • Arvid A. Danielson
Illustrator • Susan E. Wright
Administrative Services, Typography • Anne S. LoPresti
European Production Manager • Dick Leeksma

Bulk Rate
U.S. Postage
Paid
Hewlett-Packard
Company

208107JOHNAAABLACAAA 165

MR C A BLACKBURN
JOHN HOPKINS UNIV
APPLIED PHYSICS LAB
JOHNS HOPKINS RD
LAUREL MD 20810

CHANGE OF ADDRESS: To change your address or delete your name from our mailing list please send us your old address label (it peels off). Send changes to Hewlett-Packard Journal, 1501 Page Mill Road, Palo Alto, California 94304 U.S.A. Allow 60 days.